LNGS/GEO-01/06
September 2006

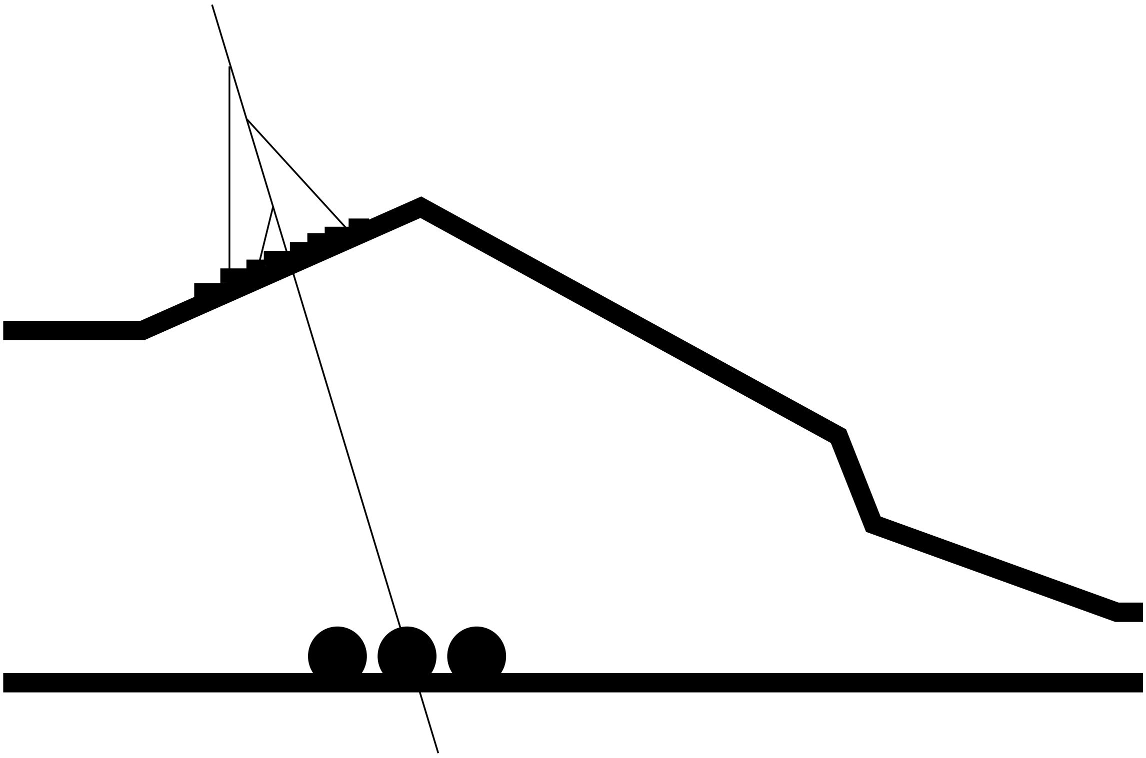

Characteristics of the Gran Sasso INFN laboratory groundwater (inferred from 1996-1998 spot sampling data) to fine-tune the conceptual model of water-rock interaction in carbonate aquifers

Raffaele Adinolfi Falcone[a], Antonella Falgiani[a], Marco Petitta[b] and Marco Tallini[c]

INFN - Laboratori Nazionali del Gran Sasso

INFN - Istituto Nazionale di Fisica Nucleare
Laboratori Nazionali del Gran Sasso

LNGS/GEO-01/06
September 2006

Characteristics of the Gran Sasso INFN laboratory groundwater (inferred from 1996-1998 spot sampling data) to fine-tune the conceptual model of water-rock interaction in carbonate aquifers

Raffaele Adinolfi Falcone[a], Antonella Falgiani[a], Marco Petitta[b] and Marco Tallini[c]

[a] *INFN - Laboratori Nazionali del Gran Sasso, S.S 17/bis, Km 18+910, 67010 Assergi (L'Aquila) - Italy*
[b] *Department of Earth Sciences, "La Sapienza" University of Rome, Piazzale A. Moro, 5, 00185 Roma - Italy*
[c] *Department of Structural, Water and Soil Engineering, University of L'Aquila, Monteluco di Roio, 67040 L'Aquila - Italy*

Abstract

The chemistry of the Gran Sasso groundwater was investigated by comparing data on drainage groundwater sampled from the underground INFN laboratory from 1996 to 1998 to data on groundwater sampled during the excavation of the motorway tunnels in the 1970s and 1980s and from the main springs. The investigation made it possible to fine-tune models of groundwater circulation in carbonate aquifers and namely of complex water-rock interactions in the unsaturated zone.

This basic hydrochemical characterisation was preliminary to plan and install a network for monitoring the quality of the groundwater drained into the INFN laboratory. Today this pilot monitoring network is already in place and starts working.

The sampled groundwater was found to be of bicarbonate alkaline-earth type and with very low mineralisation, because they did not significantly interact with

the carbonate aquifer upon their fast flowing through the unsaturated zone before sampling. Transition to more magnesic or more calcic terms was observed. Flow from NW to SE was demonstrated by the fact that the groundwater sampled at the entrance of the INFN laboratory was more mineralised than those collected in the interferometer area. Furthermore, a good correlation was noted between rainfall at the Isola del Gran Sasso climatic station and concentration of some hydrochemical parameters.

1 Introduction

The Gran Sasso carbonate massif summarizes the interactions between underground structures (motorway tunnels and INFN lab) and groundwater resources. Programs of research on vulnerability of the Gran Sasso aquifer to pollution, as well as hydrogeological and hydrochemical investigations on the groundwater flowing near the INFN underground lab, have been conducted for many years.

These activities, promoted by the "Consorzio di Ricerca Gran Sasso" and INFN, contributed to: i) improving the knowledge of quality and quantity of the INFN lab groundwater, through spot sampling of major elements and several minor ones, as well as of microbiological components; ii) characterising the basic hydrochemistry of the local groundwater; iii) identifying the lab sites to be monitored; iv) selecting suitable instrumentation, methods and physico-chemical parameters to be measured; and, finally, v) plan the installation of a groundwater quality monitoring network. After appropriate calibration steps, a pilot monitoring network was installed at the lab entrance (Teramo side) in 2005. Since then, the network has been collecting data on T, pH, electrical conductivity and other chemical species.

2 Hydrogeological outline of Gran Sasso massif

The Gran Sasso massif holds a carbonate aquifer of about 700 km^2 with well-defined hydrogeological boundaries [6], [12], [13]. The massif is one of the most representative ones of central and southern Italy, as it contains a huge groundwater resource. This resource, which is exploited for human consumption, interacts with underground structures (motorway tunnels and INFN underground lab) [1], [2], [3], [14], [15], [22], [23], [27], [31], [35]. Indeed, 30% of all the drinking water of the Abruzzi region originates from the Gran Sasso hydrogeological system. The environmental value of the massif has been recognised since 1991, when it was designated as a natural park. Many of its spring areas give rise to major wetlands, some of which are now protected by regional laws.

Inside the Gran Sasso aquifer, minor groundwater divides (corresponding to faults or lithological boundaries) obstruct but do not prevent groundwater from flowing, so much so that the Gran Sasso can be define as a partitioned karst aquifer.

The Gran Sasso hydrogeological system is composed of Meso-Cenozoic carbonate units (reservoir unit - aquifer) and bounded by Miocene sandstones, marls and clays (impermeable unit - aquiclude) along its northern side and by Quaternary fluvial and lacustrine deposits (conglomerates, breccias, sands and clays) (aquitard, i.e. semi-impermeable unit) along its southern side (Fig. 1).

The Gran Sasso karst aquifer accommodates a unique wide regional groundwater (hydraulic gradient: 5-20 per thousand). At its border, the groundwater feeds springs with high discharge values (more than 1 m^3/s each), which are located at low altitude along its southern side. The groundwater also supplies other springs (mean discharge: 0.1-0.5 m^3/s each), located at high altitude along its northern and eastern sides.

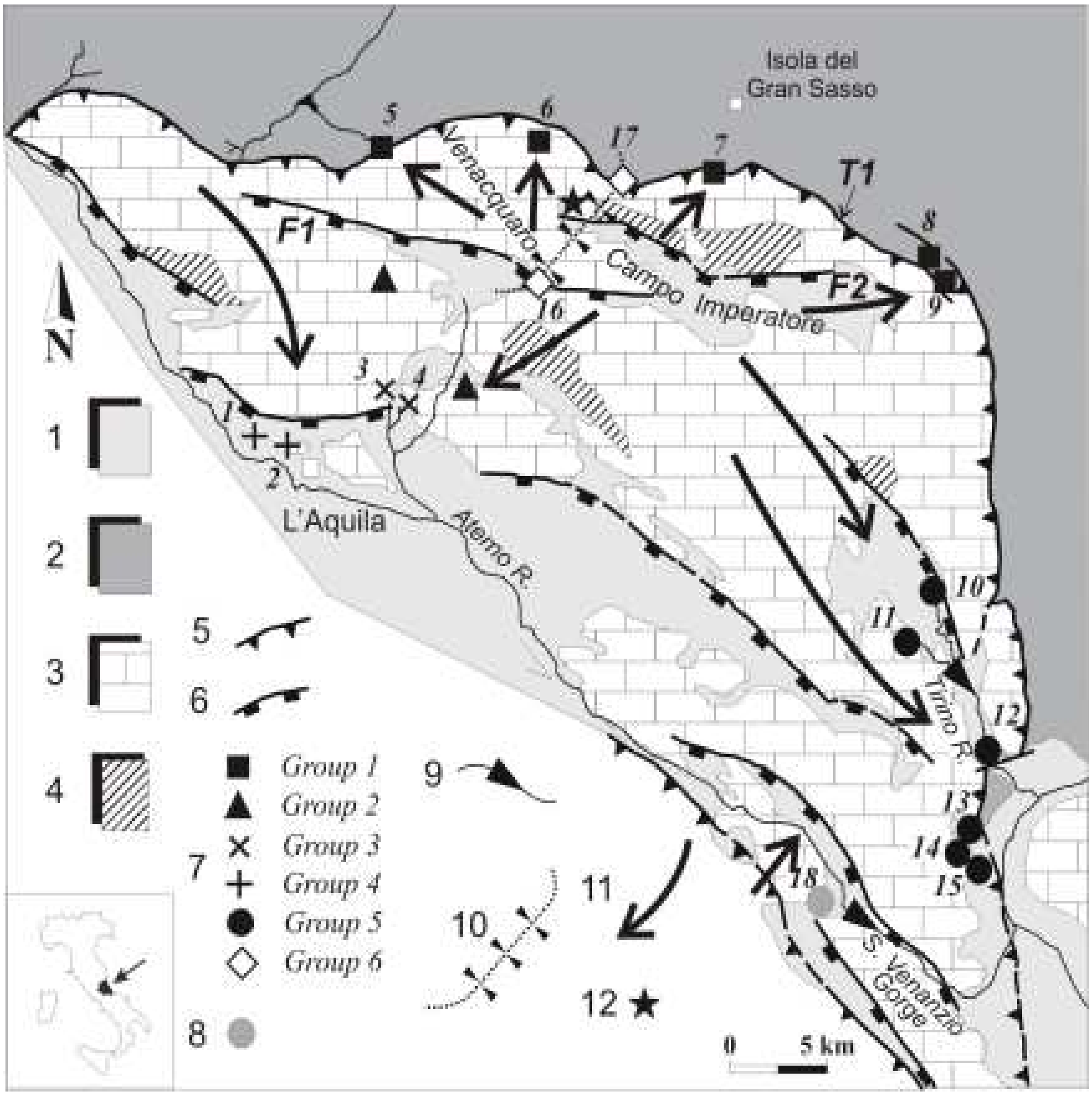

Figure 1: Gran Sasso hydrogeological system (partly modified from [4]). 1 - aquitard (continental clastic deposits of intramontane basins, Quaternary); 2 - aquiclude (terrigenous turbidites, Mio-Pliocene); 3 - aquifer (carbonatic sequences of platform - reef included - and slope to basin lithofacies, Meso-Cenozoic); 4 - low permeability substratum (dolomite, upper Triassic); 5 - overthrust (Gran Sasso regional overthrust: T1); 6 - normal fault (Valle Fredda Fault: F1, Fontari Fault: F2); 7 - main spring (symbols refer to the six spring group identified in the Gran Sasso): 1 - Vetoio; 2 - Boschetto; 3 - Tempera; 4 - Vera; 5 - Chiarino; 6 - Rio Arno; 7 - Ruzzo; 8 - Vitella d'Oro; 9 - Mortaio d'Angri; 10 - Capo d'Acqua; 11 - Presciano; 12 - Basso Tirino; 13 - S. Calisto; 14 - S. Liberata; 15 - Capo Pescara; 16 - L'Aquila side underground drainage; 17 - Teramo side underground drainage; 8 - Molina Aterno spring group (18) related to Sirente hydrogeological system; 9 - linear spring; 10 - highway tunnel drainage; for the hydrogeological section see figure 2; 11 - presumable groundwater flowpath; 12 - INFN underground lab.

The total discharge of the Gran Sasso springs is about 23 m^3/s, corresponding to a net infiltration of more than 800 mm/year [6], very high with respect to an average rainfall of about 1,200 mm/year [34]. Rainfall has decreased significantly since 1980 [33], obviously reducing net infiltration and consequently spring discharges [21].

The high value of net infiltration is to be related to intense carbonate rock jointing and faulting, epikarst features, underground conduits and climate.

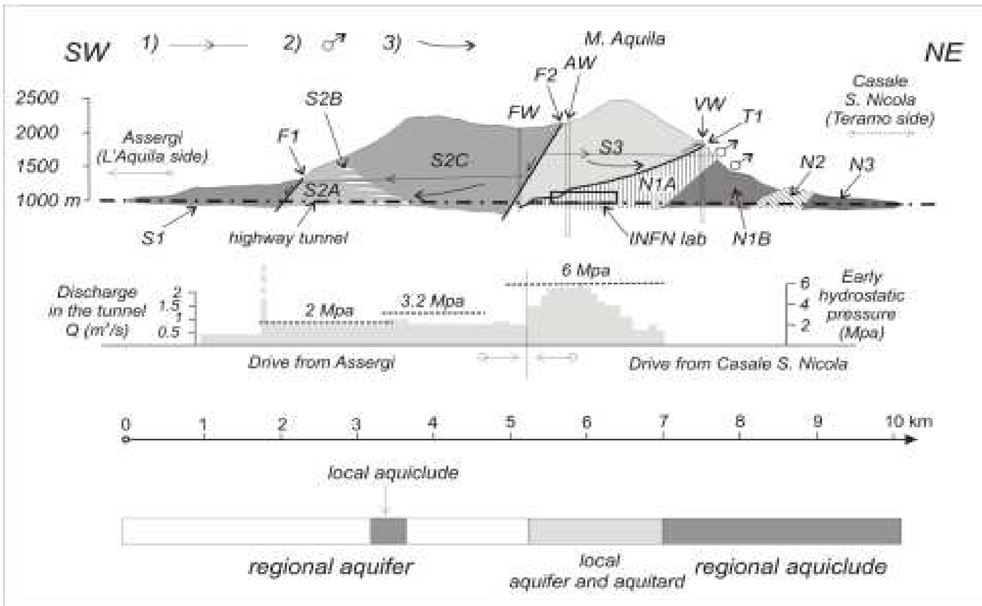

Figure 2: Gran Sasso hydrogeological section in the direction of the motorway tunnels (for location, see Fig. 1). 1 - water table before tunnel excavation; 2 - spring (group 1); 3 - groundwater flow. Zones with different hydrogeological behaviour are shown (abbreviations are those used in the text) (modified from [14] and [22]).

The area has 12 main springs, lying at the border of the massif and in contact with impermeable deposits (Figs. 1, 2, 3 and Tab. 1) and having a discharge of about 23 m^3/s [24]. The springs were gathered into 6 groups, based on groundwater circulation and hydrochemical characteristics [30]; [36], [19]. The springs of group 1 are situated on the northern slope, at an elevation of over 1,000 m and with a discharge of 2 m^3/s. They are related to outflow from the top part of the regional groundwater, which is caused by a thrust fault. This fault, which acts as a hydraulic threshold, puts the carbonate aquifer (i.e. hangingwall) in contact with terrigenous formations (i.e. footwall) [18], [16].

The springs of group 2, located at high elevation, have a fluctuating and low discharge, because they are fed by local porous perched aquifers, consisting of Quaternary slope, fluvial or glacial deposits overlying the carbonate bedrock.

The principal springs of the Gran Sasso massif lie in its southern area (L'Aquila plain - group 4: [32]; and Tirino River valley: [29] - group 5), at an elevation of less than 650 m. Their total discharge is 17 m^3/s, which adds to the one of Capo Pescara (7 m^3/s), supplied

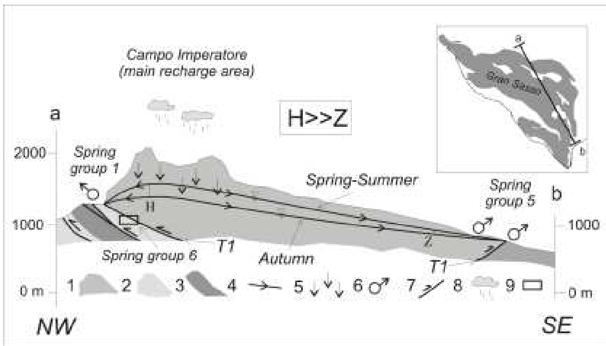

Figure 3: Hydrogeological section (not in scale) of the different seasonal contributions of water-rock interaction in the Gran Sasso carbonate aquifer, along a NW-SE direction (partly modified from [4]). In the proposed model, water table variations influence the hydrochemical characteristics of groundwater. 1- regional aquifer; 2- local aquifer; 3- regional aquiclude; 4- water table; 5- vertical groundwater movement in the unsaturated zone; 6- spring; 7- regional thrust fault T1 (no-flow boundary); 8- main recharge contribution; 9- INFN lab; H is higher than Z.

Spring group	*Spring*	*Elevation (m a.s.l.)*	*Mean discharge (1994-2000) (m^3/s)*	*Mean discharge before tunnel construction (m^3/s)*
1	Chiarino	1315	**0.05**	0.08
	Rio Arno	1524	**0.19**	0.30
	Ruzzo	750-1660	**0.33**	0.57
	Mortaio d'Angri	650	**0.14**	0.28
	Vitella d'Oro	690	**0.18**	0.38
3	Tempera	650	**0.79**	1.20
	Capo Vera	650	**0.19**	0.50
4	Vetoio	640	**0.44**	0.70
	Boschetto	625	**0.22**	0.22
5	Capodacqua	340	**2.80**	5.00
	Presciano	336	**1.95**	2.00
	Basso Tirino	300	**5.50**	5.40
	S.Calisto	300	**2.00**	1.80
	Capo Pescara	270	**6.70**	7.50
6	Tunnel L'Aquila side	970	**0.45**	0
	Tunnel Teramo side	970	**1.05**	0

Table 1: Gran Sasso main springs: discharges measured in 1994-2000 and before motorway tunnel construction (reported from [14]).

in part by the nearby Sirente aquifer [25]. The Tempera and Vera springs, having a total discharge of 1 m^3/s, belong to group 3 ([28]). They show evidence of fast circulation in karst conduits directly connected to the aquifer core (i.e. Campo Imperatore, tectono-karstic highplain being the preferential recharge area of the Gran Sasso).

These springs, together with those of group 1 (Teramo side), lie close to and in axis with the motorway tunnels. Consequently, they are the ones which suffered the most from construction of the tunnel, as their discharge decreased.

Finally, the groundwater sampled from the tunnels (group 6) is characterised by low water-rock interaction and so by low salinity ([26]).

In effect, this groundwater only flows vertically in the unsaturated zone, from the preferential recharge area corresponding to the aquifer core, with fast replacement and no backwater in the aquifer. It therefore represents the least evolved and formerly hydro-chemical end member from which all other groundwater develops by centrifugal circulation from the core to the periphery, increasing groundwater flowpaths, water-rock interaction and salinity. The characterisation of this groundwater is thus crucial to fine-tuning the conceptual model of the Gran Sasso aquifer.

The differences between the six spring groups (in terms of local hydrostructural setting and hydrochemistry) support groundwater flowpaths from the core of the massif to its boundaries; these flowpaths depend on various factors, such as structural setting, karst development and evolution, outcrops of dolomite bedrock, local recharge effects and geological setting near the springs.

In the proposed hydrogeological model, groundwater flows from recharge areas (concentrated at the core of the aquifer) to springs, moving from the centre (preferential recharge area: Campo Imperatore plateau, elevation 1,700 m) to the boundaries of the massif and reaching remote springs. Along the way, salinity and temperature, which are complicated by the local structural and geological setting, increase. Many faults and thrusts generate local groundwater divides, enabling groundwater to flow between adjacent sectors and to seep into and from the aquifer boundary [4], [5], [18].

Moreover, seasonal recharge induces vertical fluctuations of the water table, which is high in late Spring-early Summer and low in Autumn.

Vertical water movement in the lower part of the unsaturated zone and horizontal movement in the water-table zone are hypothesised. Consequently, the longer the groundwater flowpaths (i.e. the lower the spring elevation), the longer are the residence time, the more intense is water-rock interaction and, accordingly, the higher is groundwater mineralisation (Fig. 3).

Discharge from Gran Sasso springs and rivers measured before tunnels excavation and consequently groundwater drainage from tunnels (1970'-1980') were higher than the same discharge measured after the tunnels excavation. But in recent years (1996-2000), discharge has risen slightly. Probably the decrease is due not only to tunnel drainage, but also to climate variations [31].

Groundwater level monitoring at the borders of the karst aquifer can improve the understanding of the relations between such aquifer with Quaternary alluvial aquifers and aquitards. In the L'Aquila Plain, groundwater flows from the Gran Sasso aquifer to the multilayered aquifer of the plain, to its main springs and to the Aterno River. In the Tirino Valley, Quaternary alluvial deposits prevent groundwater to follow the same path [31].

3 Hydrogeological setting of the motorway tunnels and the INFN underground laboratory

In the motorway tunnel area, the massif can be concisely described as consisting of: i) a southern block, mostly made up of carbonate rocks (regional aquifer); these rocks are the hangingwall of the Gran Sasso thrust front (T1, Fig. 2); and ii) a northern block, which is practically the footwall of the thrust fault (T1) and which accommodates calcareous-siliceous-marly rocks (local aquifer and aquitard) and arenaceous-calcarenitic-clayey rocks (regional aquiclude) (Fig. 2) ([7]).

Useful hydrogeological data were obtained upon excavations for the motorway tunnels. Based on these data and on other data from three wells (Fontari, M. Aquila and Vaduccio), the tunnel area was divided into homogeneous sectors (Fig. 2) [1], [8], [9].

S1 (progressive distance - L'Aquila side - PDLS - : from 400 to 2,000 m): "southern aquifer". Boring of the tunnel met the regional aquifer from PDLS 1,300 m (maximum discharge of 250 L/s, piezometric level a few metres above the excavation level).

S2A (PDLS: from 2,000 to 3,180 m): "lower aquifer". When crossing the Valle Fredda fault (F1, Fig. 2) and its adjacent sector, a high-pressure aquifer was met; this aquifer is supported by the cataclastic belt of the fault and contained inside the carbonate complex. The northern boundary of this aquifer is marked by poorly permeable calcareous-marly layers. At the time of the excavation, the hydrostatic level lay about 200 m above the tunnel. During tunnel boring, the overall discharge from this sector of the aquifer was equal to approximately 250 L/s.

S2B (PDLS: from 3,180 to 3,630 m): "aquitard". This sector has outcrops of marly and calcareous-marly terms of Mesozoic age; however, these terms are not a major obstruction to groundwater flow.

S2C (PDLS: from 3,630 to 4,950 m): "upper aquifer". Carbonate formations in this sector (separated from the previous sector by a fault) represent another excellent aquifer. In the initial portion of this sector, about 200 L/s were drained. A well drilled in this area was reported to drain until 1991, at a pressure of roughly 10 atmospheres, corresponding to an upper piezometric level about 100 m above the excavation level. The following carbonate formations are less productive in the sector which is closest to the fault, at PDLS 3,630 m.

S3 (PDLS: from 4,950 to 5,170 m): "dolomitic aquifer". This short sector has a paramount importance; indeed, above the tunnel level, it corresponds to the Monte Aquila area, with carbonate rocks (limestones, dolomitic limestones and dolomites) which are thrust over calcareous and calcareous-marly terms. This sector extends from the Fontari fault (F2) to the main thrust fault (T1). Near the Fontari fault (F2), dolomitic rocks have a very thick cataclastic belt acting as an important permeability boundary. This belt explains why, in the upward sector and at the time of the excavation, the hydrostatic level was much higher than in sector S2C, at a depth of approximately 1,600 m. The dolomitic complex proved to be poorly permeable at depth, whereas groundwater flows were concentrated in the area closer to the Fontari fault (F2). The regional thrust fault (T1) is encountered in the westernmost area of the lab, near the interferometer, where the groundwater under study was sampled.

N1A (PDLS: from 5,170 to 7,100 m): "northern aquifer": in addition to the thrust fault T1, the tunnel also features the overturned limb of a syncline having its core in the siliceous-calcareous-marly formations. Near the thrust fault, no particular hydrogeological problems were encountered. Inside the carbonate terms ("Calcare massiccio" formation) at depth, the hydrostatic level was the same as in sector S3 and lay about 600 m above the excavation level. It is worth stressing that, in this particular setting, the thrust fault at the tunnel level does not represent a significant permeability boundary. Actually, the Gran Sasso regional aquifer also extends beyond the thrust fault, where permeable carbonate terms occur. However, its further advance is restrained by impermeable terrigenous terms, which lie at the core of the syncline and which play the role of aquiclude (no flow boundary) at depth for the entire Gran Sasso aquifer. In this sector, where excavation proceeded from the northern side, the drained discharges exceeded 1,000 L/s on average, with peaks close to 2,000 L/s. Transition to impermeable terrigenous terms takes place according to a overturned stratigraphic sequence, which is complicated by a number of minor faults. The groundwater sampled at hall A and at the entrance of the INFN lab (Teramo side) originates from this sector.

N1B (PDLS: from 7,100 to 7,800 m); "northern aquiclude". The tunnel crosses a syncline composed by terrigenous lithologies which have practically no groundwater.

N2 and N3 (PDLS: from 7,830 to 10,150 m). This is the terminal sector of the motorway tunnel, which always crosses practically impermeable terrigenous terms. Here, these terms form a much less tectonised sequence with marly and calcareous intercalations at its base. The stratigraphic sequence repeats in the terminal sector N3, with an anticline having its core in the marls; local groundwater with low discharge potential is present.

This description along the axis of the tunnel is supplemented with data from three wells (Fontari, M. Aquila and Vaduccio), which were drilled before boring of the tunnel.

The most relevant hydrogeological finding from the well data is the occurrence of a highly permeable palaeo-karst belt lying at an elevation of about 1,600 m and having a thickness of 50 to 100 m [9], [27]. This interval corresponds to the fluctuations of the hydrostatic level before tunnel boring. At depth, at the height of the tunnel, rocks are instead less permeable and this justifies both the high piezometric level and the volume of water flows into the tunnel, owing to a high hydraulic gradient.

Additional data on the tunnel area come from the different amounts of drainage which were recorded at the same point in the two separate tunnels: the left one and the right one (the left one more westerly and the right one more easterly) [1], [20]. In the first section of groundwater interception, in sector S1 (PDLS from 1,300-2,000 m), groundwater mostly flowed in the right tunnel. Investigations, made at a later stage (early 1990s) for completing of the INFN underground lab, confirmed the larger flow of groundwater in the right tunnel (about 260 L/s vs. 210 in the left one).

For sector S2, no direct data on drainage into the two tunnels are available. Studies carried out in 1991 showed that overall drainage on the Assergi side was larger in the right tunnel [20]. Differential measurements (only made in the left tunnel) indicated a discharge of about 60-70 L/s from sector S2C, of about 75-85 L/s from sector S2A and another 60 L/s from the aquifer in sector S1. Actually, also sector S3 is likely to contribute to drainage, although it has a very low permeability.

As to the Teramo side, the groundwater drained into the two tunnels (practically at PDLS from 5,400 to 7,100 m) is diverted and exploited for drinking uses by the drinking water supply company of Teramo Province. In addition to this drainage, water certainly overflowed from the intake structure until the 1980s. At present, practically all of the tunnel waters are diverted and exploited. The amount of groundwater draining into the tunnels adds to the one into the underground lab area (which started at the end of 1984). Of the latter discharge (about 200 L/s), approximately half flows directly into the drains of the tunnel area (especially into the left tunnel, corresponding to the lab area) and the remaining part takes a separate path and reaches the Casale S. Nicola outlet, where it meets the water overflowing from the aqueduct intake structure.

With regard to the water contributions from the two tunnels (from sector S1A, i.e. from the overturned sequence of limestones making up the footwall of the regional thrust-fault - T1, Fig. 2), the left tunnel contributed more (on average 750 vs. 650 L/s from the right tunnel) until construction of the lab (1977-1984). Actually, drainage into the INFN lab only affected drainage into the left tunnel, whose decrease was practically equivalent to the overall drainage into the INFN lab.

This suggests two key considerations:

a) excavations for construction of the INFN lab did not intercept new portions of the aquifer, but actually diverted water which previously drained into the left tunnel (Fig. 4);

b) the waters drained into the left tunnel are recharged by the western side of this sector of the Gran Sasso aquifer, while the groundwater drained into the right tunnel mostly comes from the eastern side but from a sector having a lower piezometric level.

It is worth emphasising that the higher amount of groundwater drained into the left tunnel gives insight into the main direction of water flow in the area under undisturbed conditions (i.e. before construction of the tunnel), i.e. from W to E. This finding is consistent with hydrodynamic assumptions about the entire hydrogeological system. On these assumptions, groundwater flows from the Venacquaro-Campo Imperatore sector towards the more depressed south-eastern one and then towards the low-altitude springs of Tirino and Popoli (group 5).

Another important element obtained from the data on drainage on the Teramo side is that discharge gradually declined from 1979 at least through 1990. The first period of decline was predicted and justified by the emptying of one portion of the aquifer as a result of the new hydrodynamic setting arising from construction of the tunnel (5-6 years). However, with the achievement of a new hydrodynamic equilibrium in the regional aquifer, progressive stabilisation of discharge was expected. Therefore, the further drop in drainage can be correlated with lower recharge of the aquifer, resulting from the lower precipitation which was recorded on average in the same period [21], [33].

The assumption that the dominant recharge is from the left part of the tunnels is validated by the fact that the decrease in discharge (observed in the 1980s) is almost entirely attributable to the right tunnel. Indeed, if the main direction of recharge of the waters drained into the tunnels were from W, any general decrease in piezometric levels caused by lower recharge would be reflected more in the sector hydraulically located downstream of the assumed drainage, i.e. in the right tunnel. The groundwater coming from W would anyway be intercepted by the lab-left tunnel drainage, without recording significant variations. Conversely, drainage into the right tunnel of waters that would naturally flow eastwards, would sharply drop owing to the lowering of the piezometric surface.

4 Structural setting and rock jointing in the lab area

In sum, the groundwater sampled near the interferometer drains dolomitic rocks of the upper Trias, which constitute the hangingwall (sector S3, Fig. 2) of the thrust fault (T1, Fig. 2). In contrast, the groundwater sampled at hall A, exit and entrance of the INFN lab drains well-bedded micritic calcareous rocks with and without intercalations of marls of Scaglia type and of massive detrital calcareous material. These Cretaceous rocks have an overturned strike direction (N 0^o-30^o) and dip direction eastwards by 40^o-60^o. They represent the overturned limb of a syncline, highly dislocated by secondary faults, which characterises the footwall (sector N1A, Fig. 2) of the thrust fault T1 (Fig. 2). Chemistry of groundwater is highly conditional upon the rocks from which they were sampled.

In the lab area, three main families of secondary faults were identified [11]: one of extensional type (N45^oW), dipping by 50^o-60^o especially in the Scaglia-like formation; another one, always extensional (N60^o-90^oE), dips northwards by 20^o-30^o (abnormal values under the classical Anderson's model of fault origination, suggesting rotation and tilting; this fault is located near the thrust fault T1 towards the area of the interferometer (Figs. 3 and 4); a third family of variably-oriented dextral strike-slip faults is located in the NW sector of the INFN lab and in conduit no. 8 (Fig. 4). In the rocks of the INFN lab, stylolitic cleavage is very widespread, especially in the Scaglia-like formation, and a 5 to 20 m-thick fault rock zone occurs in the upper Jurassic limestones which lie in immediate contact with the thrust fault T1 (Figs. 2, 4 and 5).

The thrust fault and associated rock, the attitude of the strata with marly intercalations and the stylolitic cleavage of the T1 footwall rocks are all elements transversal to the E-W direction of water flow, as inferred from data collected upon excavations for construction of the INFN lab. These elements would hinder groundwater circulation more or less significantly; and yet, the consistent orientation of the main secondary faults (NW-SE- and E-W- trending) favours and thus plays a significant role in groundwater circulation. Furthermore, density of jointing is likely to affect the amount of groundwater discharge.

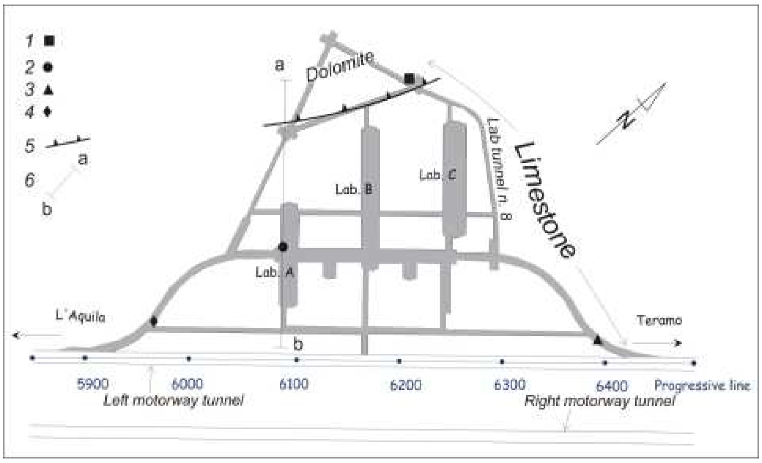

Figure 4: Gran Sasso INFN underground lab with sampling sites (1: interferometer; 2: hall A; 3: lab entrance; 4: lab exit); 5: regional thrust fault T1; 6: geological section of Fig. 5 (partly modified from [14]).

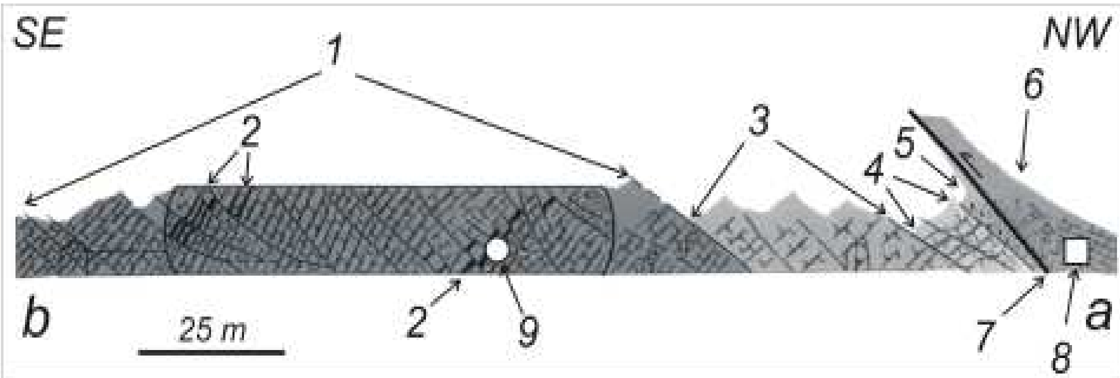

Figure 5: Local geological section of the Gran Sasso INFN underground lab (for location, see Fig. 4). 1- Scaglia-like stratified cherty micritic limestone (Upper Cretaceous); 2- blackish marls intercalated with Scaglia-like limestone (Upper Cretaceous); 3- bioclastic limestone (Upper Cretaceous); 4- stratified cherty micritic limestone (Lower Cretaceous); 5- massive detrital limestone with infrequent cherty nodules (Upper Jurassic); 6- dolomite (Upper Triassic); 7- regional thrust fault; groundwater sampling sites: 8- interferometer (site location projected in the section); 9- hall A (partly modified from [11]).

5 Hydrochemical data

The LNGS environmental lab carried out the majority of the hydrochemical analyses on the INFN lab groundwater. The groundwater was sampled above all from 1996 to 1998 and spot sampled from 1987 to 1993 and from 2003 to 2005 in four sites: at the lab entrance and exit (Teramo side), at hall A and near the interferometer (Figs. 4 and 5).

The main hydrochemical parameters that were measured were pH, electrical conductivity at 20^{o}C, DR at 110 ^{o}C, major elements (Ca, Mg, Na, K, HCO_3, SO_4, Cl) and SiO_2 and, for characterising the bicarbonate component, total CO_2, alkalinity and total hardness in ^{o}F.

To assess the possible degree of pollution, NO_3, NO_2 and NH_4 were also measured; heavy metals, such as Pb, Fe, Mn, Sn, Ni, Zn, Al, B and Ba, were measured only at intervals.

6 Instrumentation and analytical methods

Table 2 displays the analytical methods which were adopted.

parameter	Adopted analytical method
pH	2060 IRSA-CNR APAT vol 1
El cond T=20°C	2030 IRSA CNR APAT vol. 1
Alkalinity	2010 met. B IRSA CNR APAT vol. 1
Total CO_2	Distillation in presence of sulphuric acid and N_2 gas flow, absorption on barite and retrotitration with HCl with known titre
Total hardness	2040 met. B IRSA CNR APAT vol. 1
DR (T=110°C)	Gravimetric method
Al	3050 met. B IRSA CNR APAT vol. 1 - 3000 IRSA CNR APAT vol. 1 (ECOS)
Ba	3050 met. B IRSA CNR APAT vol. 1 - 3000 IRSA CNR APAT vol. 1 (ECOS)
B	Graphite hot-plate AAS - 3050-A1 IRSA CNR 100 (ECOS)
Ca	3130 met A IRSA CNR APAT vol. 1 - 2040 IRSA CNR APAT vol. 1 (ECOS)
Fe	3160 met. B IRSA CNR APAT vol. 1 - 3160 met. A IRSA CNR APAT vol. 1
Mg	3180 met. A IRSA CNR APAT vol. 1 - 2040 IRSA CNR APAT vol. 1 (ECOS)
Mn	3190 met. B IRSA CNR APAT vol.1 - 2040 IRSA CNR APAT vol. 1 (ECOS)
Ni	3220 met. B IRSA CNR APAT vol.1 - 3000 IRSA CNR APAT vol.1 (ECOS)
Pb	3230 met. B IRSA CNR APAT vol.1 - 3000 IRSA CNR APAT vol.1 (ECOS)
K	3240 met. A IRSA CNR APAT vol.1 - 3000 IRSA CNR APAT vol.1 (ECOS)
Cu	3250 met B IRSA CNR APAT vol.1 - 3000 IRSA CNR APAT vol.1 (ECOS)
Na	3270 met. A IRSA CNR APAT vol.1 - 3000 IRSA CNR APAT vol.1 (ECOS)
Sn	3280 met. B IRSA CNR APAT vol.1 - 3000 IRSA CNR APAT vol.1
Zn	3320 met B IRSA CNR APAT vol.1 - 3000 IRSA CNR APAT vol.1
NH_4	4030 met. A2 IRSA CNR APAT vol.2
NO_2	4050 IRSA CNR APAT vol.2
Cl	Spectrophotometric method at 440 nm - 4020 IRSA CNR APAT vol.2 ((ECOS)
SIO_2	4130 IRSA CNR APAT vol.2
SO_4	4140 met. B IRSA CNR APAT vol.2 - 4020 IRSA CNR APAT vol.2 (ECOS)

Table 2: Analytical methods adopted for spot sampling of the INFN lab groundwater in the 1996-1998 period.

Use was made of a Perkin Elmer Lambda 18 UV-visible spectrophotometer and of a Perkin Elmer 3110 flame and graphit oven atomic absorption spectrometer, together with more common units, such as pHmeter, analytical balance, conductimeter, etc.

At the present time (November 2005), the underground LNGS environmental lab consists of the following instrumentations:

1. teflon system for water sampling;
2. system for filtering 20 μm particles;
3. Torton-Mettler probes for measuring temperature, pH and electrical conductivity;
4. DIONEX ion chromatograph composed of three modules for quali-quantitative analysis of alkaline, earth-alkaline and transition elements and anions: LC 20, AD 50 and AD25;
5. TOC meter (model 2244AP Sievers);
6. gas chromatograph for mass spectrometry (GC/mass/mass VARIAN 4000, equipped with Purge and Trap sample concentrator XPT) with TOC warning;
7. high-efficiency liquid chromatograph (LC/MS/MS Q TRAP - Applied Biosystems) connected to an HPLC Perkin Elmer series 200 equipped with Diode Array Detector and TOC warning;
8. Gilson sampling system with TOC warning;
9. CADAS 200 Dr Lange UV-visible spectrophotometer.

These units were assembled to build a pilot monitoring network, which is being calibrated. The network measures the TOC of discharge waters every 6 minutes. The TOC pilot instrumentation is designed to issue a pre-alert or an alert when reaching TOC concentrations of 1,000 or 2,000 ppb, respectively. The alarm triggers the spectrometer system, which detects the volatile or non- volatile organic substances with the GC- or LC- spectrometer, respectively.

The TOC alarm also activates water sampling with the Gilson system, in order to separately analyse water samples out of the assembly line.

7 Collected data

The main hydrochemical parameters (Tab. 3) were measured on samples of drainage groundwater collected in three sites in the period 1996 to 1998. The waters were sampled on a monthly basis (for a total 84 sampling surveys). The sampling sites were the interferometer area, hall A, exit and entrance of the INFN lab (Figs. 3 and 4). Data from spot sampling surveys conducted in 1987-1993 and 2003-2006 were also considered (Tab. 3).

Parameters	N° data				Mean				Max. value				Min. value				Dev. St.			
pH	6$^{(1)}$	5$^{(2)}$	59$^{(3)}$	70$^{(4)}$	8.21$^{(1)}$	8.37$^{(2)}$	8.26$^{(3)}$	*8.27*$^{(4)}$	8.44$^{(1)}$	8.50$^{(2)}$	8.50$^{(3)}$	8.50$^{(4)}$	7.50$^{(1)}$	8.32$^{(2)}$	8.04$^{(3)}$	7.50$^{(4)}$	0.35$^{(1)}$	0.07$^{(2)}$	0.12$^{(3)}$	0.15$^{(4)}$
El. Cond. (T= 20°C)	6	7	58	72	105	118	95	*98*	117	144	138	144	92	100	78	78	9	18	13	15
Dry Residue (T= 110°C)	6	5	50	63	78	83	77	*79*	102	86	101	108	78	78	64	64	9	4	6	8
Ca	6	8	48	64	20.75	20.68	17.98	*18.64*	22.00	22.60	20.50	22.60	17.20	16.72	15.40	15.40	1.87	2.01	0.90	1.67
Mg	6	8	48	64	11.26	10.20	10.70	*10.60*	12.00	11.30	14.00	14.00	8.10	9.90	9.00	8.10	1.28	0.46	1.23	1.20
Na	6	5	58	71	1.57	0.87	0.54	*0.63*	2.00	1.00	0.85	2.00	0.55	0.47	0.45	0.45	0.49	0.23	0.06	0.24
K	4	6	56	68	0.40	0.36	0.16	*0.20*	1.00	0.62	0.35	1.00	0.30	0.24	0.12	0.12	0.34	0.14	0.04	0.13
HCO_3	1	3	55	60	103.70	102.80	101.70	*101.83*	103.70	103.70	103.70	103.70	103.70	101.00	97.60	97.60	---	1.56	1.97	1.95
Cl	5	7	59	72	1.99	1.25	1.01	*1.07*	1.80	1.80	1.30	1.80	1.10	0.90	0.70	0.70	0.32	0.30	0.16	0.23
NO_3	5	6	58	70	1.75	0.88	0.84	*0.85*	1.00	1.10	1.39	1.39	0.70	0.70	0.13	0.13	0.11	0.17	0.18	0.17
SiO_2	5	6	47	58	1.80	1.04	0.90	*0.93*	1.10	1.10	1.11	1.11	0.50	0.92	0.50	0.50	0.27	0.07	0.10	0.12
CO_2	0	1	44	46	---	25	45	*45*	---	25	59	59	---	25	25	25	---	---	7	8

Table 3: Main hydrochemical parameters of groundwater sampled in 1996-1998 (electrical conductivity in μS/cm, concentration in mg/L) in the INFN Gran Sasso lab: (1) - Teramo side lab entrance; (2) - hall A; (3) - interferometer area; (4) - total data, i.e. sum of data of sites 1, 2 and 3. (^{o}) data sampling: 23 Nov. 2005, 27 Dec. 2005, 13 Feb. 2006, 27 Feb. 2006, 21 March 2006; (*) data sampling: 27 Dec. 2005.

51 of these analyses proved to be complete and were regarded as reliable, as the charge balance ($\Delta\%$) expressed as

$$\Delta = \frac{\sum cations - \sum anions}{\sum cations + \sum anions}$$

was below the 6% threshold value, as specified in official standards.

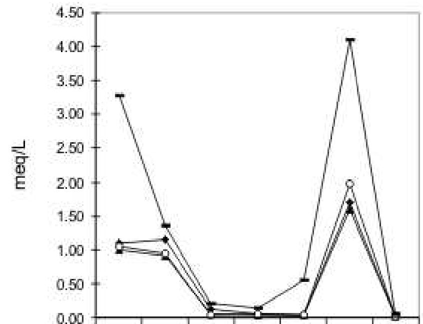

	Ca	Mg	Na+K	Cl	SO4	HCO3	NO3
lab exit	1.10	1.15	0.11	0.05	0.04	1.70	0.02
lab entrance	1.00	0.91	0.05	0.04	0.03	1.60	0.01
Assergi Plant	1.04	0.95	0.04	0.05	0.03	1.98	0.03
Capo Pescara	3.28	1.35	0.20	0.14	0.54	4.10	0.05

Figure 6: Schoeller's diagram: hydrochemical characteristics of groundwater sampled in the INFN lab (lab exit on 23 Nov. 2005 and lab entrance on 27 Dec. 2005) compared to those of the groundwaters of Assergi plant (sampled in November 2001) and Capo Pescara spring (sampled in November 2001), which is the most mineralised one of entire Gran Sasso massif. DR of INFN lab exit and entrance, Assergi plant and Capo Pescara is 102, 91, 163 and 378, respectively.

The waters are classified as oligomineral, since their DR ranges from 108 to 64 with an average of 79 mg/L. Schoeller's diagrams (Fig. 6) and pie charts (Fig. 7) infer that the waters are classified as bicarbonate alkaline-earth and in particular calcic-magnesic. Water hardness expressed in French degrees (°F) goes from 8.40 and 8.50 at the interferometer and hall A to 10.67 and 10.40 at the entrance and exit of the INFN lab. Hardness also varies over time. Indeed, at the entrance of the INFN lab, the 1987-1988 surveys indicated an average of 9.73, while those of 2005-2006 gave a value of 10.67. Spatio-temporal changes in hardness are consistent with the previously described conceptual model of groundwater circulation in the lab area.

In general, the groundwater sampled in the INFN lab (located at the core of the aquifer) comes directly from their preferential recharge area (plateau of Campo Imperatore and internal valleys of the Gran Sasso chain, i.e. Venacquaro and Rio Arno) by flowing rapidly through the unsaturated zone. This fact, i.e. poor water-rock interaction, explains its low mineralisation. This groundwater represents the non-chemically-evolved primitive end member, from which all the Gran Sasso spring waters gradually evolve as, through centrifugal underground drainage from the core to the periphery of the aquifer, underground flowpaths and residence times and water-rock interactions increase (Fig. 3). Schoeller's diagrams (Figs. 6 and 8) display the data of the groundwater sampled in the INFN lab vs. those from other significant springs of the Gran Sasso: concentrations gradually increase in spring waters vs. the primitive groundwater of the INFN lab; all of them keep their alkaline-earth properties, although INFN lab groundwater has a higher percentage of Mg (group 6).

At present, considering that the tunnels were completed around the early 1980s, the lab groundwater only interacts with the rocks of the unsaturated zone (sector S3 and 1A, Fig. 2) and with those of the INFN lab (Figs. 4 and 5) before being sampled. Active drainage without stagnation inside the rocks of the INFN lab affects the characteristics of these waters: low mineralisation (Tab. 3 and Fig. 6), strong undersaturation in calcite (Figs. 9-13) and dolomite, and relationship with an open system with respect to CO_2 content (Fig. 14). The Tillmans diagram (Fig. 9) shows that the groundwater sampled in the INFN lab lies in the calcite undersaturation range.

Fig. 10 evidences that the waters sampled in the INFN lab after tunnel boring are clearly undersaturated in calcite, testifying active drainage and no stagnation in the aquifer. In particular, the groundwater sampled at the interferometer is more undersaturated than those collected at hall A and at the entrance and exit of the INFN lab (Figs. 4, 5, 11 and 12). This finding may be attributed to shorter travel and thus shorter residence time and lower water-rock interaction of the interferometer groundwater than those of other groundwater (see later). At any rate, the groundwater sampled during tunnel boring (1972) in the Valle Fredda fault low-permeability rocks (F1, Fig. 2) was saturated, as evidenced by the good alignment of the data along the calcite saturation curve; water stagnation and water-rock interaction are also clear.

In contrast, the diagram of Fig. 14 shows that CO_2 concentration is independent of pH, demonstrating that the system is open, i.e. with a continuing contribution of CO_2 given by groundwater of unsaturated zone.

Basic chemistry of the investigated groundwater is obviously related to carbonate reservoir rocks, as displayed in the Ca vs. HCO_3 diagram; the diagram shows the calcite and dolomite saturation curves and the range of variability of CO_2 pressure in air (0.003 bar) and in soil (0.15 bar) (Fig. 15). The average values of Ca and HCO_3 concentrations of the main springs and of groundwater sampled in the tunnel (Tab. 4) have an excellent correlation (0.86) (Fig. 16). The regression curve has the same angular coefficient as the calcite saturation curve but is shifted onto the Mg-calcite range, suggesting that the latter minerals are clearly responsible for dissolution.

The values of groundwater sampled in the INFN lab is lower, because they refer to hydrochemically primitive groundwater. This groundwater results from deep and fast active drainage, which only takes place in the unsaturated zone. They lie along the dolomite saturation curve, because the rocks from which they were collected have a strong dolomitic component (Figs. 4 and 5). Furthermore, the value of the groundwater sampled in the INFN lab (16, 17, 18 of Fig. 16) lies in the partial CO_2 pressure range that is typical

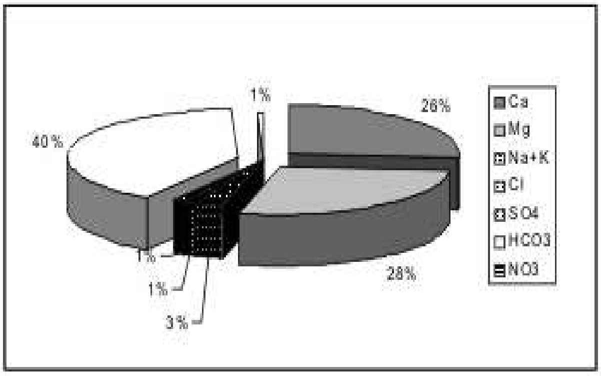

Figure 7: Pie chart of groundwater sampled on 23 Nov. 2005 at the exit of the lab.

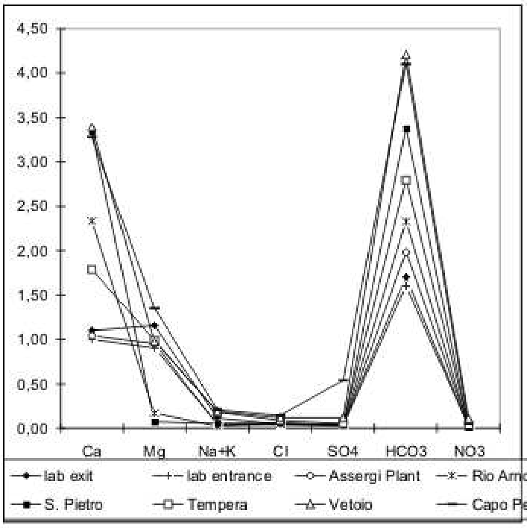

Figure 8: Schoeller's diagram: hydrochemical characteristics of groundwater sampled in the INFN lab (lab exit on 23 Nov. 2005 and lab entrance on 27 Dec. 2005) compared to those of the groundwater of the Gran Sasso massif as classified in Fig. 1: lab exit and entrance and Assergi plant: group 6; Rio Arno: group 1; S. Pietro: group 2; Tempera: group 3; Vetoio: group 4; Capo Pescara: group 5.

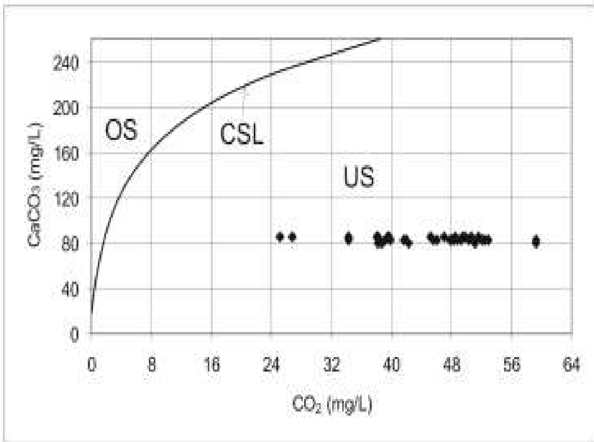

Figure 9: $CaCO_3$ vs. CO_2 diagram (the so-called Tillmans diagram): groundwater sampled in the INFN lab (period: 1996-1998). CSL: calcite saturation curve; OS: oversaturated water; US: undersaturated water.

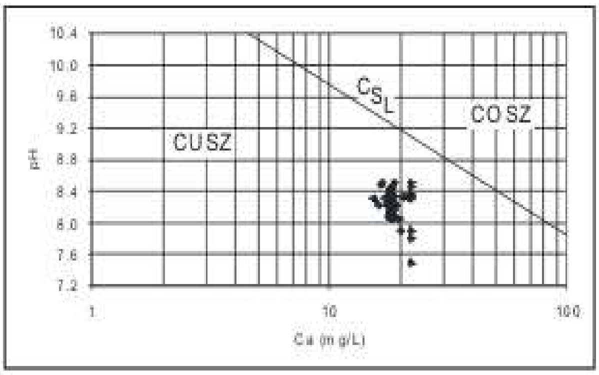

Figure 10: pH vs. Ca diagram: calcite undersaturated groundwater from the INFN lab (1987-2005 period). CSL represents the calcite saturation curve at T = 10^{o}C, CUSZ: calcite undersaturation zone, COSZ: calcite oversaturation zone.

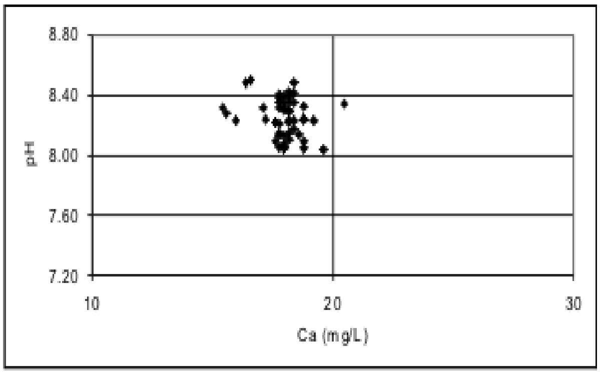

Figure 11: pH vs. Ca diagram: calcite undersaturated groundwater sampled in 1996-2003 from the interferometer site.

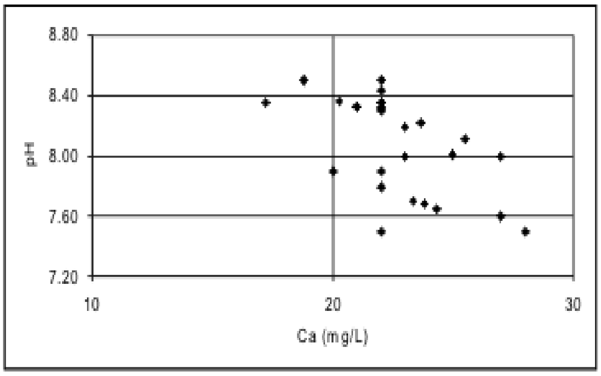

Figure 12: pH vs. Ca diagram: calcite undersaturated groundwater sampled in 1987-2004 from the lab entrance and exit, hall A, "drainage chamber" (right tunnel - L'Aquila side: progressive distance 5,000 m) and Teramo side underground drainage.

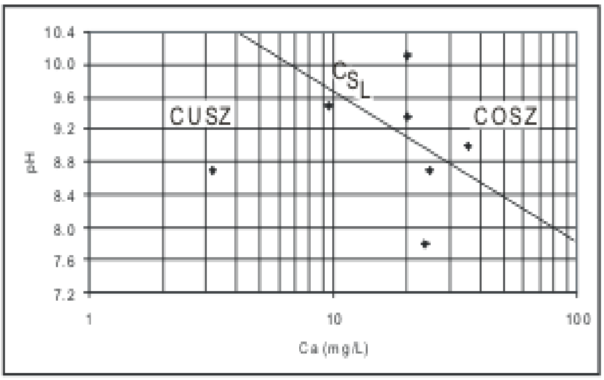

Figure 13: pH vs. Ca diagram: calcite saturated groundwater sampled in 1972 from the tunnel (L'Aquila side): progressive distance 1,480-1,980 m (Valle Fredda Fault zone (F1, Figs. 1 and 2). CSL represents the calcite saturation curve at T = 10^{o}C, CUSZ: calcite undersaturation zone, COSZ: calcite oversaturation zone.

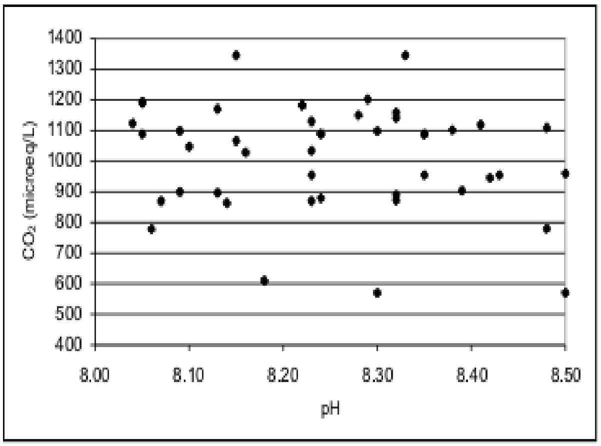

Figure 14: CO_2 (μeq/L) vs. pH diagram of groundwater sampled in the interferometer area (1996-1998 period).

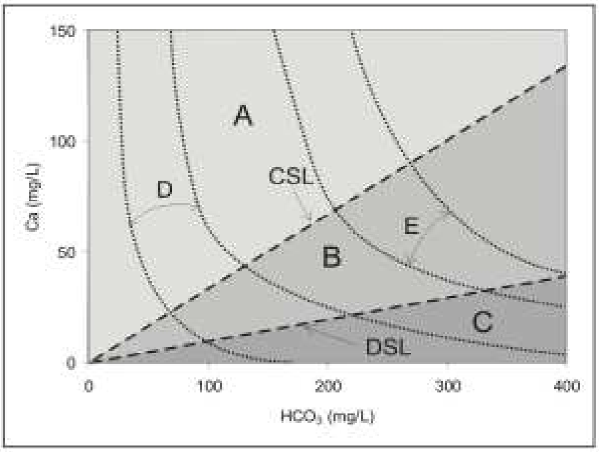

Figure 15: Ca vs. HCO_3 diagram which is presented in the following figures. CSL: calcite saturation curve; DSL: dolomite saturation curve; field A: area of undersaturation of calcite, Mg-calcite and dolomite; field B: area of undersaturation of Mg-calcite and dolomite and of oversaturation of calcite; field C: area of oversaturation of calcite, Mg-calcite and dolomite; areas between the dotted lines represent CO_2 pressure in air (D) and in soil (E), which is equal to 0.003 and 0.15 bar, respectively (from [10]).

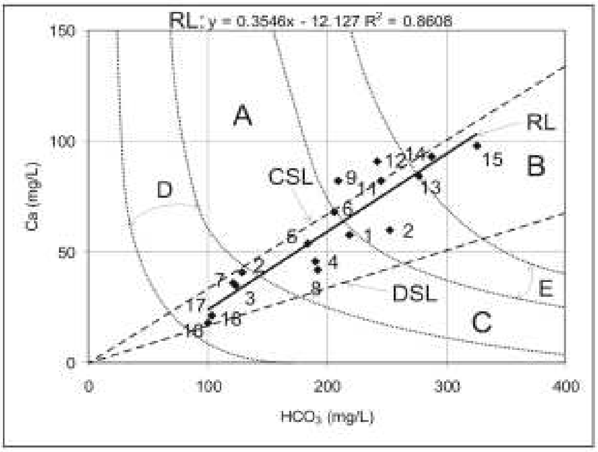

Figure 16: Ca vs. HCO_3 diagram showing the data (Tab. 3) of the main Gran Sasso springs compared to those of groundwater sampled in the INFN lab (16, 17, 18). For the meaning of letters, see Fig. 15. RL: regression curve of total data.

Spring group	*spring*	*N° of reference*	*time of sampling*	*data*	*HCO3 (mg/L)*	*Ca (mg/L)*
Group 1	Chiarino	1	2001	3	219	58
	Rio Arno	2	2001	3	129	41
	Ruzzo	3	2001	3	124	35
	Mortaio d'Angri	4	2001	3	190	46
	Vitella d'Oro	5	2001	2	184	54
Group 2	S. Pietro	6	2001	3	206	68
Group 3	Tempera	7	1996-97	7	122	36
	Vera	8	2001	2	192	42
Group 4	Vetoio	9	1996-97	7	209	82
	Acqua Oria	10	2001	2	252	60
Group 5	Capo d'Aqua	11	1996-97	6	245	82
	Presciano	12	2001	7	242	91
	S.Liberata	13	1996-97	7	277	84
	S.Calisto	14	1996-97	7	288	93
	Capopescara	15	1996-97	7	326	98
Group 6	Interpherometer	16	1996-98	45	101	18
	Room A	17	1997	3	104	21
	Entrance lab (Teramo side)	18	1987	1	104	21

Table 4: Data reported in Fig. 16. Spring group as presented in Fig. 1. Data of 2001, 1996-1997 and of group 6 from [4], [35], and from the environmental lab of LNGS-INFN, respectively.

of air, substantiating the assumption that this groundwater is rapidly drained through an unsaturated zone which is very thick (actually it is over 1,000 m-thick).

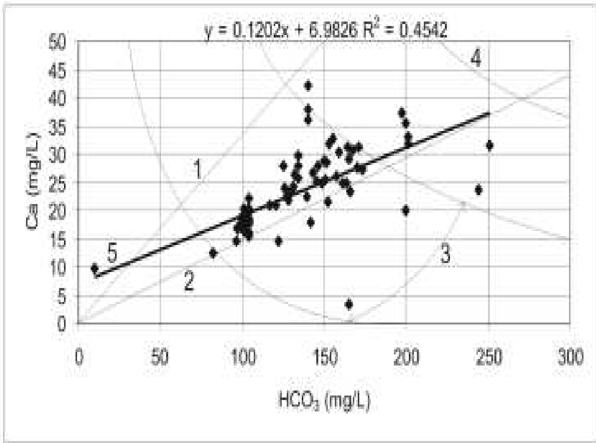

Figure 17: Ca vs. HCO_3 diagram: total data of groundwaters sampled in the tunnel and INFN lab (1971-2006 period). 1: calcite saturation curve; 2: dolomite saturation curve; areas representing CO_2 pressure in air (3) and in soil (4), which is equal to 0.003 and 0.15 bar, respectively; 5: regression curve of total data of groundwaters sampled in the tunnel and INFN lab (1971-2006 period).

Among others, the Rio Arno and Ruzzo springs (group 1) on the Teramo side and the Tempera springs (group 3) on the L'Aquila side (the closest ones, supplied by the regional aquifer and lying in axis with the tunnels) show pairs of values that are very similar to those of the groundwater sampled in the INFN lab. This fact points to a direct linkage between the aquifer core and these springs. The dolomitic rocks in the interferometer area (base of the stratigraphic sequence of sector S3, Fig. 2) influence the chemistry of the waters sampled in the INFN lab, as shown by Figs. 17 and 18 and by Mg/Ca ratio and electrical conductivity variations (Figs. 19 and 20). Indeed, in Fig. 17, the linear regression of all the available data is aligned towards the dolomite regression curve. The average values of Ca - HCO_3 pairs for the waters sampled in the INFN lab and in the tunnels before and after their boring (Tab. 5 and Fig. 18) are sharply aligned along the dolomite saturation curve and show concentrations varying vs. time. Indeed, the value of the waters sampled in the drainage chamber (at approximately 5,000 m on the L'Aquila side) before tunnel boring (value 2, Fig. 18) is higher than the one after tunnel boring (value 5, Fig. 18). This means that tunnel boring altered both groundwater residence time and groundwater-rock interactions. In other words, before tunnel boring, groundwater stagnated more inside the aquifer, thus interacting more with local rocks and becoming more mineralised than after tunnel boring. In effect, after construction of the tunnel, the sampled groundwater reflects fast and active drainage which is related to their movement inside the unsaturated zone only.

The groundwater sampled at the interferometer, compared to those of hall A, entrance

sampling site	*N° reference*	*Time of sampling*	*HCO$_3$ (mg/L)*	*Ca (mg/L)*
Tunnel (progressive distance from L'Aquila side: 1980-2050-2110 meters) ("Valle Fredda fault zone")	1	1971-72	17	
			169	28
			54	10
			242	39
Tunnel (progressive distance from L'Aquila side: 3000-5000 meters)	2	1972-77	19	
			149	26
			16	5
			56	18
Tunnel (progressive distance from Teramo side: 0-1000 meters)	3	1974-80	5	
			116	21
			34	8
			86	18
interferometer	4	1996-98	44	
			101	18
			2	1
			4	4
"Drainage room– exit lab" (progressive distance from L'Aquila side: 5900 meters)	5	2001-2004	5	
			127	23
			4	1
			7	1
Tunnel drainage: Teramo side	6	2001-2006	4	
			133	23
			53	1
			21	3
Assergi plant for drinkable groundwater	7	2004-2006	3	
			146	26
			4	1
			7	1

HCO$_3$ (mg/L)	*Ca (mg/L)*
data number	
average	average
st dev	st dev
amplitude	amplitude

Table 5: Ca and HCO_3 concentrations reported in Fig. 18.

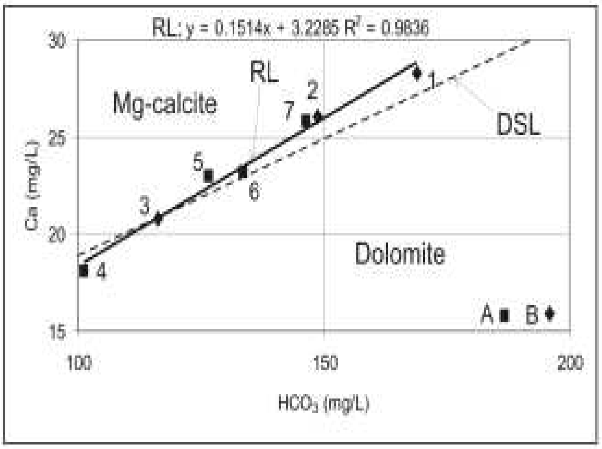

Figure 18: Ca vs. HCO_3 diagram: average data of groundwater sampled in different sites of the tunnel and lab areas over time (see Tab. 5). Groundwater sampling during (A) and after (B) tunnel excavation; RL: regression curve of plotted data; DSL: dolomite saturation curve.

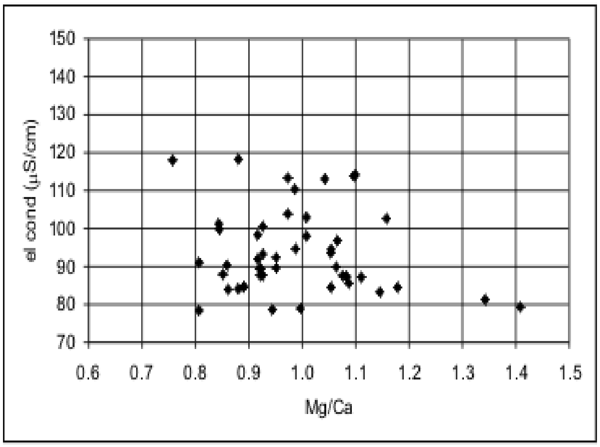

Figure 19: Electrical conductivity vs. Mg/Ca diagram: data of groundwater sampled in the interferometer site.

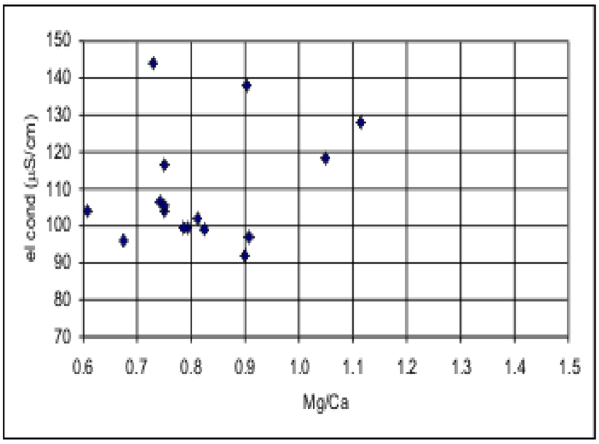

Figure 20: Electrical conductivity vs. Mg/Ca diagram: data of groundwater sampled at hall A, exit and entrance of the INFN lab.

and exit of the INFN lab, is relatively more enriched in Mg than in Ca and less mineralised (lower electrical conductivity and DR, Figs. 19 and 20). This is due to the fact that dolomitic rocks only lie in the interferometer area, whereas micritic or finely detrital calcareous rocks are dominant in the lab area. Moreover, proceeding from NW to SE along an ideal transversal line from the more internal areas (interferometer) to the more external areas of the INFN lab (hall A and thus entrance of the INFN lab), HCO_3, Na, K, Cl, NO_3, SiO_2 and electrical conductivity sharply increase with a concurrent decrease in the Mg/Ca ratio (Figs. 21 and 22). Taking into account the discharge variations recorded during construction of the INFN lab and the hydrological budget of the nearby Rio Arno spring groundwater basin, the above findings corroborates the assumption of underground drainage in the laboratory area from NW to SE. Therefore, the groundwater sampled at hall A and entrance of the INFN lab is though to have covered a longer distance inside calcareous rocks than the groundwater drained through the dolomites of the interferometer area. As a result, the former are likely to be much more mineralised and with a lower Mg/Ca ratio than the latter.

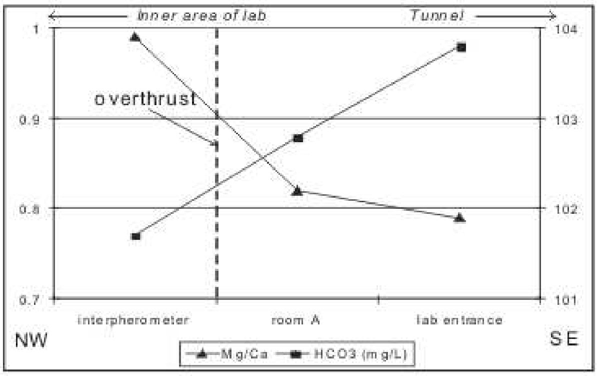

Figure 21: Changing Mg/Ca (Y-axis: left side) and HCO3 concentration (Y-axis: right side) from the inner to the outer part of the INFN lab.

Based on the always gradual concentration and electrical conductivity variations from NW to SE, the regional thrust fault (T1 in Figs. 2, 4 and 5) in the interferometer area does not appear to act as a hydrodynamically impermeable barrier but is in fact neutral to groundwater circulation.

The values of NO_3 and of Cl, measured at the entrance of the INFN lab, proved to be higher. However, NO_3 was definitely below the indicative value of 5 mg/L and the maximum admissible concentration of 50 mg/L under the applicable Italian legislation. Cl is likely to derive from salts, such as the calcium chloride used to lower the temperature of ice formation on roads. These values are probably due to the fact that more external areas, such as the entrance and hall A, are more exposed to contamination by human activities with respect to the more internal ones, such as the interferometer area.

The hydrochemical variations of the groundwater sampled monthly or bi-weekly (in a series extended to 1996-1998) in the interferometer area were correlated with monthly precipitation at the Isola del Gran Sasso climatic station. The station lies close to the presumable recharge area of the portion of aquifer corresponding to the location of the INFN underground lab. A reverse correlation in the January-August period and a direct one in the October-December period were observed between the average concentration of HCO3 (Fig. 23), Cl (Fig. 24), Ca/Mg ratio (Fig. 25) and electrical conductivity (Fig. 26) and average monthly precipitation (Fig. 27). The reverse correlation (in the January-August period) may be due to the fact that new recharge waters exert a dilution effect on the concentration of chemical species in old (previously infiltrated) groundwater. The direct correlation in the Autumn period is instead to be attributed to failed recharge of the aquifer owing to snowfall: water remains blocked at the surface and can seep into the aquifer only after thawing, i.e. in Spring. Regarding Ca/Mg ratio variations and dilution phenomena associated with aquifer recharge, it is clear that diluted waters become enriched in cations (e.g. calcium), which are bound to more soluble salts (e.g. calcite), and not in magnesium, which is bound to dolomite, a less soluble salt. In particular, over a shorter timescale, the aquifer response to new recharges is more complex. Indeed, sampling surveys from late October 1997 to early February 1998 (Figs. 28 and 29) indicate peak rainfall in October 1997 (256 mm), subsiding in subsequent months. This peak rainfall brings about dilution of concentrations, which continues in November, December and January. The aquifer responds to the new recharge (corresponding to the travel time inside the unsaturated zone) in about 15 days. The time gap between peak rainfall in October and peak values of electrical conductivity and Ca/Mg ratio (adequately reverse correlated) may be due to the so-called "piston effect". Otherwise expressed, under a conceptual model of propagation of a flood peak in a fissured karst aquifer, the new groundwater pushs volumes of older and thus more mineralised groundwater towards the deepest zones of the aquifer, causing first a hydrochemical peak and then a discharge peak (Fig. 30). An additional effect is the increase in the volumes of groundwater that are generated by the peak rainfall event (October 1997). This groundwater saturates aquifer fissures (joints, faults, strata, etc.) and naturally amplifies leaching and mineralisation processes. Gradual electrical conductivity and Ca/Mg ratio variations during the three months following the peak rainfall event infer that groundwater flows in a medium that is definitely fissured but with few karst conduits, which may instead favour fast drainage and minimise rock leaching. Prior to the peak rainfall event, fissures are not totally saturated. Nevertheless, with the input of new volumes of water into the aquifer, due to propagation of the peak rainfall event, all the fissures become saturated, thereby enhancing water-rock interactions and thus water mineralisation.

8 Main results

The hydrochemical characteristics of drainage groundwater, sampled in four specific sites of the Gran Sasso INFN underground lab, were investigated. The samples had been

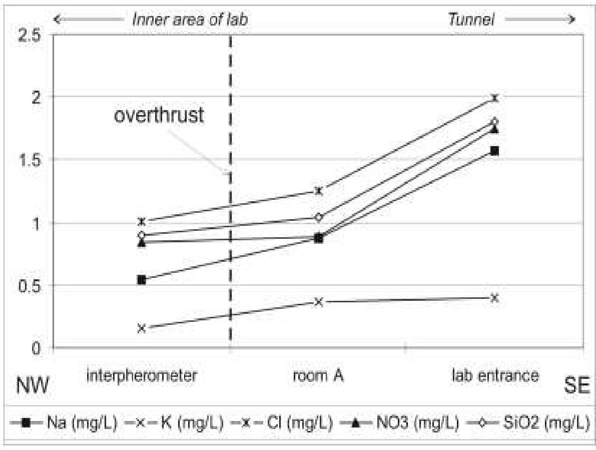

Figure 22: Changing average concentrations of Na, K, Cl, NO_3 and SiO_2 from the inner to the outer part of the INFN lab.

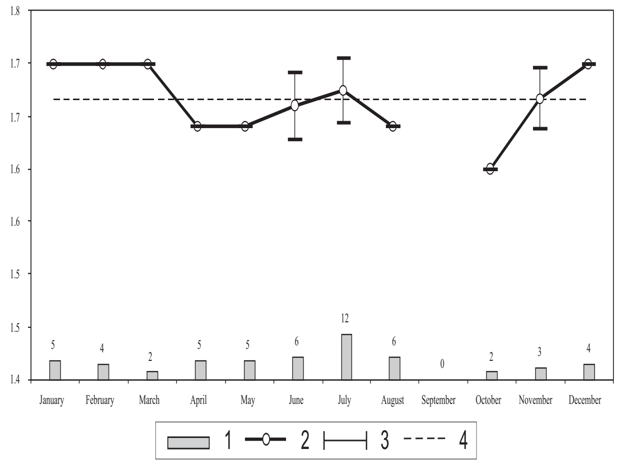

Figure 23: Monthly HCO_3 concentrations (interferometer site - 1996-1998 period). 1- monthly frequency of data; 2 - monthly average; 3 - standard deviation of monthly value from yearly average; 4 - yearly average.

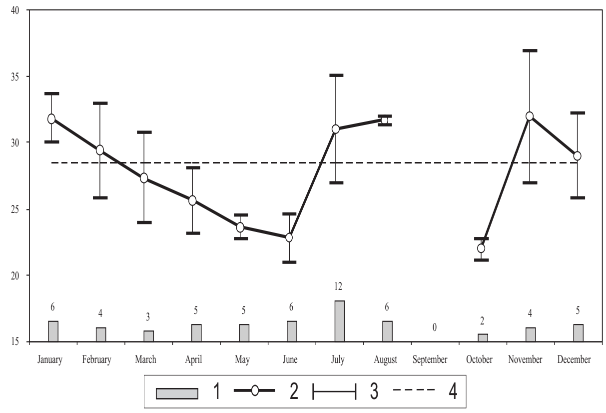

Figure 24: Monthly Cl concentrations (interferometer site - 1996-1998 period). 1- monthly frequency of data; 2 - monthly average; 3 - standard deviation of monthly value from yearly average; 4 - yearly average.

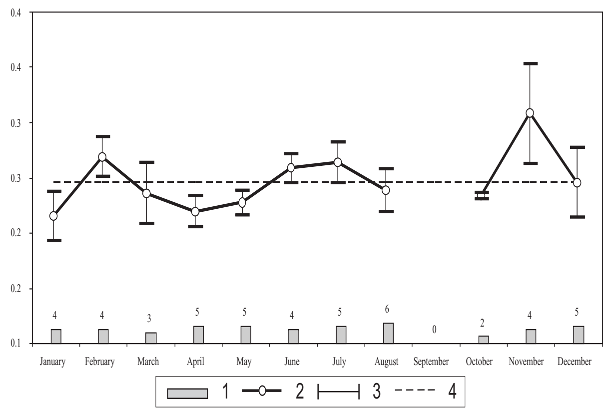

Figure 25: Monthly Ca/Mg ratios (interferometer site - 1996-1998 period). 1- monthly frequency of data; 2 - monthly average; 3 - standard deviation of monthly value from yearly average; 4 - yearly average.

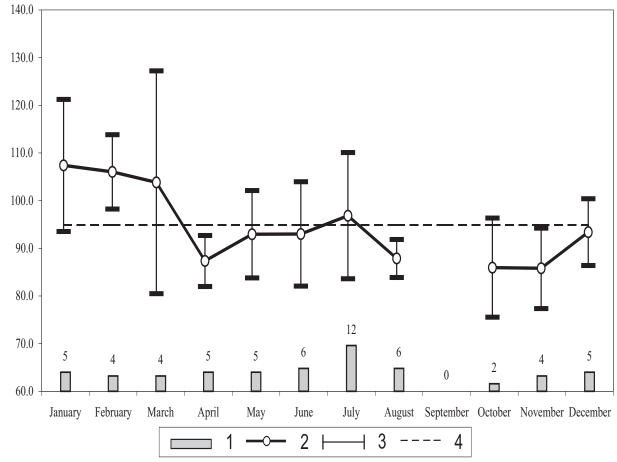

Figure 26: Monthly electrical conductivity (μS/cm at 20^{o}C) (interferometer site - 1996-1998 period). 1- monthly frequency of data; 2 - monthly average; 3 - standard deviation of monthly value from yearly average; 4 - yearly average.

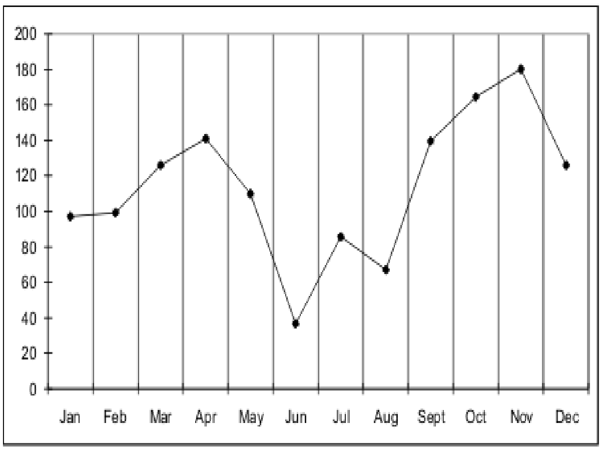

Figure 27: Average monthly rainfall in mm for the 1996-1998 period, recorded at the Isola del Gran Sasso climatic station.

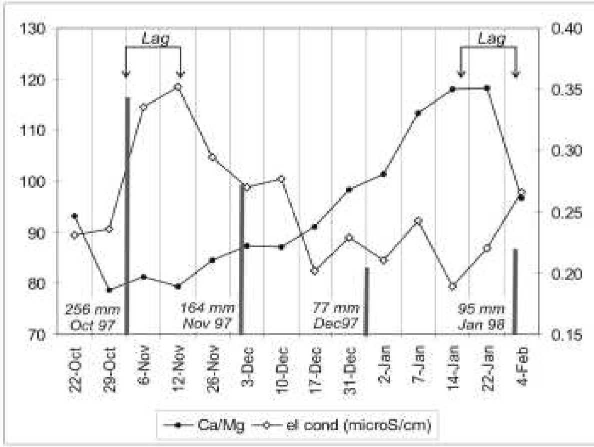

Figure 28: Ca/Mg and electrical conductivity vs. time (from October 1997 to February 1998) data from interferometer site. Monthly rainfall recorded at the Isola del Gran Sasso climatic station. Note the reverse correlation between electrical conductivity and Ca/Mg ratio; the lag between maximum rainfall and maximum or minimum value of electrical conductivity and Ca/Mg ratio, respectively, is about 15 days.

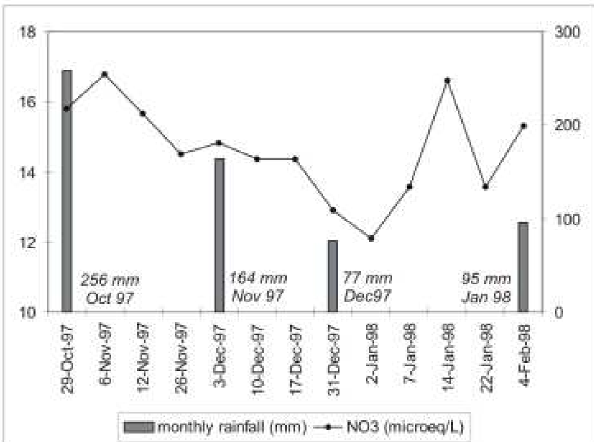

Figure 29: NO_3 vs. time: data from interferometer site.

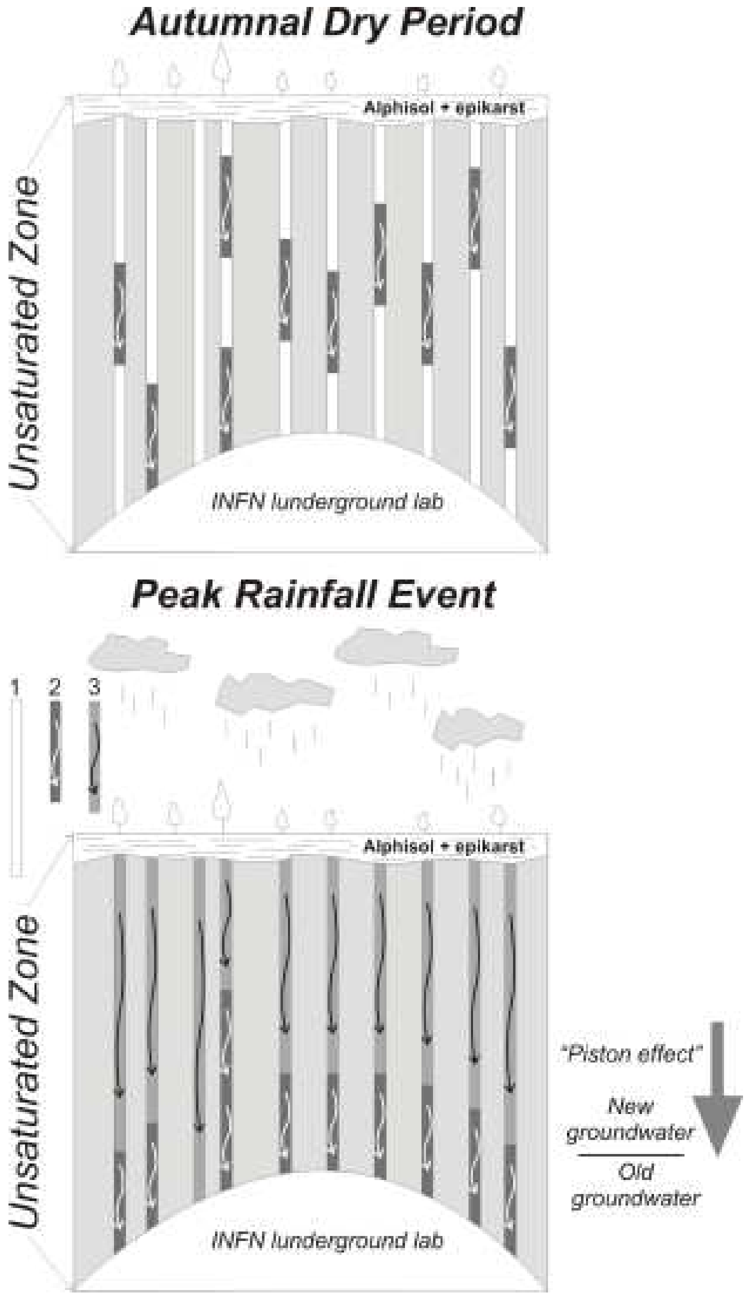

Figure 30: Section not in scale representing groundwater infiltration into the unsaturated zone before and during or after a peak rainfall event like the one of October 1997 (see Fig. 28); this event is characterised by the "piston effect" (new and less mineralised infiltrating groundwater pushes the old and more mineralised one into the fractures, causing a shift of the hydrochemical peak with respect to the hydrological one). The unsaturated zone is 1,400 m thick, soil and epikarst only few meters. 1- fracture without infiltrating groundwater; 2- old and more mineralised infiltrating groundwater; 3- new and less mineralised infiltrating groundwater related to the peak rainfall event.

collected on a monthly or bi-weekly basis, especially in the 1996-1998 period. These data were compared to similar data obtained for the main springs of the Gran Sasso massif in the 1995-2006 period and for drainage groundwater inside the motorway tunnels during their construction in the 1970-1980 period. The study improved the understanding of water-rock interactions, recharge processes and fault response to groundwater circulation in fissured karst aquifers and namely on the most representative one of central-southern Italy, i.e. the Gran Sasso.

Major elements, as well as T, pH and electrical conductivity and - in view of the specific hydrogeological setting of carbonate aquifers - total CO_2 content were measured.

This activity was conducted, inter alia, with a view to planning a hydrochemical monitoring network (already operational in part). The network is expected to characterise the quality of groundwater flowing into the INFN lab in real time and, at the same time, to assess the vulnerability of the Gran Sasso aquifer. This aquifer, whose resources are exploited for drinking uses, also hosts underground human activities (motorway tunnel and INFN lab).

The sampled groundwater is bicarbonate calcic-magnesic, have very low mineralisation (average value: about 100 S/cm), low temperature (average value: about 5 ^{o}C) and a slightly akaline average pH (about 8.30).

Currently, these groundwater is highly undersaturated in calcite (Figs. 9 e 10) and is related to an open CO_2-H_2O-$CaCO_3$ system, as demonstrated by pH independence from total CO2 (Fig. 14). Besides, as the Gran Sasso is a carbonate aquifer, its main chemistry is obviously related to the equilibrium of carbonates/bicarbonates in water. These waters were collected from the aquifer core under conditions of active drainage and no stagnation. The cause of their very low mineralisation and strong carbonate undersaturation lies in their scarce interaction with rocks before their sampling; this interaction only occurs during their flowing down into the unsaturated zone. These primitive waters come from the main recharge area of the aquifer, which lies on the vertical line of the INFN lab. They are regarded as the end member of the Gran Sasso groundwater, from which all other waters evolve, with the increase in the number of underground flowpaths, residence time and water-rock interactions. The related model supposes centrifugal drainage from the core of the aquifer (INFN lab area) towards the periphery of the massif (Figs. 3 and 16).

Actually, the chemistry of this groundwater displays slight changes, which are likely to depend on the types of rock from which they were sampled. Therefore, the samples collected inside the upper Triassic dolomites (base of the sequence of the hangingwall of the regional thrust fault T1, Figs. 2, 3 and 5) are more clearly magnesic and less mineralised. The groundwater collected in the limestones at the exit and entrance of the INFN lab and at hall A is more mineralised and is less magnesic (Figs. 11, 12, 19 and 20). This different chemistry may be explained by the different lithologies existing in the sampling sites: dolomites in the interferometer area and limestones at hall A, entrance and exit of the INFN lab. In the first instance, less mineralisation is ascribable to the low solubility of dolomite vs. calcite. Moreover, in the special case of active drainage areas in carbonate aquifers, groundwater chemistry is reported to be highly conditional upon the rocks of the sampling area, whatever the pathways of groundwater before sampling.

Hence, water-rock interactions in the unsaturated zone are negligible vs. those occurring at the sampling point, as demonstrated also by low mineralisation.

Growing electrical conductivity and declining Mg/Ca ratio from the more internal areas (interferometer) to the more external ones of the INFN lab (close to the motorway tunnel) (Fig. 4) are attributable to longer residence times and concurrent water-rock interactions, as water pathways increase from NW to SE (from the interferometer to the tunnel). This assumption is in agreement with discharge variations measured in the tunnel and INFN lab during tunnel boring.

The rock of the regional thrust fault (T1, Figs. 1, 2, 3, 4 and 5) crossing the interferometer area has a neutral response to groundwater circulation from NW to SE (Figs. 21 and 22).

Comparing the chemistry of groundwater sampled inside the INFN lab and tunnels before and after their construction evidences a shift from more to less mineralised waters (Fig. 18) and the alignment of average values along the dolomite saturation curve.

A good correlation was observed between concentrations of some hydrochemical parameters of lab waters vs. time and rainfall (Figs. 23-27), in line with a conceptual hydrochemical model where recharge favours dilution of the concentrations of chemical species in groundwater.

An excellent correlation was also noted between rainfall, electrical conductivity and Ca/Mg ratio of lab groundwater and propagation of rainwater in the unsaturated zone in the extreme rainy period of late October 1997 (Figs. 28 and 29). In this case, the model of groundwater circulation was assumed to be the typical one of karst aquifers, i.e. a "piston effect" whereby new and less mineralised seepage waters push older and less mineralised waters into the internal part of the aquifer (Fig. 30).

The time gap between peak rainfall and hydrochemical peak is about 15 days (Figs. 28 and 29), suggesting a peak velocity of seepage into the unsaturated zone of 1,000 metres in 15 days (70 metres/day or 3 metres/hour, as reported for fissured karst media).

The hydrochemical data of the lab drainage groundwater, sampled from 1996 to 1998, were investigated and compared to other data obtained for the main Gran Sasso springs and for the groundwater sampled in the tunnels, during their construction in the 1970-1980 period. The investigation helped fine-tune or validate the conceptual models of groundwater circulation, namely of recharge processes and water-rock interactions in the unsaturated zone.

The unique location of the INFN lab, below an over 1,000 m-thick unsaturated zone in the core of an extensive carbonate aquifer, made it possible to thoroughly study complex water-rock interactions in carbonate aquifers. Furthermore, the study laid the groundwork for characterising basic chemistry of groundwater circulating inside the INFN lab and planning the sampling sites, the hydrochemical parameters to be measured and the timescales for data collection through a monitoring network. The network is expected to assess the quality of drainage groundwater in the INFN lab, which is located at the core of an aquifer, whose resources are exploited for drinking uses by intake systems in the immediate vicinity of the INFN lab.

9 Outlook for the hydrochemical monitoring

Until today, besides data acquired in 1996-98 period whose elaboration is reported in this paper, a monitoring station, located at the underground lab entrance, which analyses groundwater flowing into the lab drainage network, measures, at regular intervals of one minute, the main groundwater physical and chemical parameters as T, pH, electrical conductivity, TOC, the main hydrochemical elements and some minor ones among which Li, Sr, and Br. Moreover, on request when TOC value should exceed a safety level, the monitoring station will be able to measure and recognize, by means of high precision mass spectrometer, the principal hydrocarbons. The results reported here have permitted to plan and locate in the next future in the underground lab other four monitoring stations like the one which is now working. They will settle in the interferometer, the room A and the exit and entrance of underground lab.

10 Conclusions

The chemistry of the Gran Sasso groundwater was investigated by comparing data on drainage groundwater sampled from the underground laboratories of INFN from 1996 to 1998 to data on groundwater sampled during the excavation of the motorway tunnels in the 1970s and 1980s and from the main springs. The investigation made it possible to fine-tune models of groundwater circulation in carbonate aquifers and namely of complex water-rock interactions in the unsaturated zone.

After basic hydrochemical characterisation, a network for monitoring the quality of the groundwater drained into the INFN lab was planned to be installed and the sampling sites, hydrochemical parameters to be measured and sampling intervals were selected. A pilot monitoring network is already in place.

The sampled groundwater was found to be of bicarbonate alkaline-earth type and with very low mineralisation (electrical conductivity about 100 μS/cm), because they did not significantly interact with the carbonate aquifer upon their fast flowing through the unsaturated zone before sampling. Transition to more magnesic or more calcic terms was observed, depending on the dolomitic or calcareous composition of the rocks from which they were collected. The regional thrust fault, which separates Triassic dolomites from Cretaceous limestones, proved to have a neutral response to underground seepage from NW (more internal areas of the laboratories in which are dolomites) to SE (more external areas close to the tunnels in which are limestones). Flow from NW to SE was demonstrated by the fact that the groundwater sampled at the entrance of the INFN lab was more mineralised than those collected in the interferometer area.

Furthermore, a good correlation was noted between rainfall at the Isola del Gran Sasso climatic station (in the immediate vicinity of the recharge area of the portion of the aquifer where the INFN underground lab is located) and concentration of some hydrochemical parameters. Consequently, the time gap between peak rainfall and peak concentration of hydrochemical parameters in the drainage groundwater was estimated at roughly 15 days, whereas peak velocity of groundwater seepage into the unsaturated zone was calculated to be about 3 m/hr. This value is in line with those obtained with other methods in other Mediterranean fissured karst aquifers.

11 Acknowledgements

The authors acknowledge greatly Prof. Enrico Bellotti, chairman of the "Consorzio di Ricerca Gran Sasso", who gave us many useful suggestions and a continuous encouragement, Eng. Alberto Scaramelli, technical manager of LNGS, to review a first draft of the report, Eng. Mario Russo, head of the Abruzzi Hydrographic Department, to give us hydrological data of Gran Sasso climatic stations, Mrs. Giuseppina Giusti to help us in the chemical analysis of LNGS groundwater and Mr. Achille Bonanni for the technical support.

References

[1] ANAS-COGEFAR, Gran Sasso, il traforo autostradale. Ed. Grafiche Sefra, Milano (1980).

[2] L. Adamoli, Idrogeologia del massiccio carbonatico del Gran Sasso e conseguenze idrogeologiche degli scavi autostradali. Geologia Tecnica, **3** (1990) 4-15.

[3] V. Allocca, P. Celico, S. Fabbrocino, Grandi gallerie in realt idrogeologiche complesse. Proceedings of 1^{st} AIGA Conference, Chieti, 19-20/02/2003, (2003) 19-30.

[4] M. Barbieri, T. Boschetti, M. Petitta, M. Tallini, Stable isotopes (^{2}H, ^{18}O and ^{87}Sr/^{86}Sr) and hydrochemistry monitoring for groundwater hydrodinamics analysis in a karst aquifer (Gran Sasso, Central Italy). Applied Geochemistry, **20** (2005) 2063-2081.

[5] M. Barbieri, L. D'Amelio, G. Desiderio, A. Marchetti, T. Nanni, M. Petitta, S. Rusi, M. Tallini, Groundwater isotopic study in the Adriatic Apennine (Central Italy): a tool for the protection of karst water resources. Proceedings of 1^{st} AIGA Conference, Chieti, 19-20/02/2003, (2003) 69-81.

[6] C. Boni, P. Bono, G. Capelli, Schema idrogeologico dell'Italia Centrale. Mem. Soc. Geol. It., **35** (1986) 991-1012, with hydrogeological map at 1:500.00 scale.

[7] F. Calamita, M. Pelorosso, S. Satolli, Il ruolo dell'architettura del paleomargine mesozoico di Adria nel sistema orogenico del Gran Sasso d'Italia (Appennino centrale). Boll. Soc. Geol. It., **122** (2003) 337-349.

[8] L. Calambert, P.G. Catalano, V. Conato, L. Lambrecht, A. Monjoie, Observations dans le massif du Gran Sasso (Apennin central). C.R. Acad. Sc. Paris, **274** (1972).

[9] L. Calambert, P.G. Catalano, V. Conato, L. Lambrecht, A. Monjoie, Le sondage de Fontari dans le massif du Gran Sasso (Apennin central). C.R. Acad. Sc. Paris, **274** (1972).

[10] B. Capaccioni, O. Nesci, E.M. Sacchi, D. Savelli, F. Troiani, Caratterizzazione idrochimica di un acquifero superficiale: il caso della circolazione idrica nei corpi di frana nella dorsale carbonatica di M. Pietralata - M. Paganuccio (Appennino marchigiano). Il Quaternario, **17** (2004) 585-595.

[11] P.G. Catalano, G.P. Cavinato, F. Salvini, M. Tozzi, Analisi strutturale nei laboratori dell'I.N.F.N. del Gran Sasso d'Italia. Mem. Soc. Geol. It., **35** (1986) 647-655.

[12] P. Celico, Schema idrogeologico dell'Appennino carbonatico centro-meridionale. Memorie e Note dell'Ist. Di Geol. Appl., **14** (1979) 1-97.

[13] P. Celico, Idrogeologia dei massicci carbonatici, delle piane quaternarie e delle aree vulcaniche dell'Italia centro-meridionale: Progetti speciali per gli schemi idrici nel Mezzogiorno. Quad. Cassa Mezzog., **4/2** (1983) 1-225.

[14] P. Celico, S. Fabbrocino, M. Petitta, M. Tallini, Hydrogeological impact of the Gran Sasso motor-way tunnels (Central Italy). Giornale di Geologia Applicata, **1** (2005) 157-165.

[15] CISE - Nuova Telespazio, Realizzazione di un sistema di monitoraggio idrologico del massiccio del Gran Sasso (Progetto Idrologia): Studi Preliminari. Consorzio di Ricerca del Gran Sasso internal report, (1996) 1-444.

[16] V. Di Sabatino, M. Tallini, Valutazione dell'impatto del traforo del Gran Sasso sul sistema acquifero attraverso l'analisi del bilancio idrogeologico della sorgente Rio Arno. Proceedings of 83^{rd} Societá Geologica Italiana Meeting (Chieti, 12-16/09/2006), (2006) 213-216.

[17] V. Di Sabatino, M. Manetta, D. Sciannamblo, M. Spizzico, M. Tallini, Il radon come tracciante delle acque sorgive finalizzato alla vulnerabilit degli acquiferi carbonatici complessi: l'esempio del gruppo sorgivo del Rio Arno (Gran Sasso, Italia centrale). Proceedings of 2^{nd} Congresso Nazionale AIGA, Bari 15-17/02/2006, Giornale di Geologia Applicata, **2** (2005), 413-419.

[18] V. Di Sabatino, Manetta M., D. Sciannamblo, M. Spizzico, M. Tallini, Caratterizzazione del circuito delle acque sotterranee degli acquiferi carsici tramite lo studio del contenuto in radon delle sorgenti del Gran Sasso (Italia centrale). Proceedings of 2^{nd} Congresso Nazionale AIGA, Bari 15-17/02/2006, Giornale di Geologia Applicata, **2** (2005), 445-452.

[19] V. Di Sabatino, D. Sciannamblo, M. Spizzico, M. Tallini, Elementi minori e rapporti caratteristici delle acque sorgive del Gran Sasso (Italia centrale) per caratterizzare il

comportamento idrodinamico degli acquiferi carbonatici. Proceedings of 83^{rd} Societá Geologica Italiana Meeting (Chieti, 12-16/09/2006), (2006) 209-212.

[20] DISAT-INFN, Indagine sull'eventuale impatto idrogeologico prevedibile con la realizzazione della galleria servizi e dell'ampliamento dei laboratori sotterranei del Gran Sasso. Internal report, (1997) 1-93.

[21] W. Dragoni, Some considerations on climatic changes, water resources and water need in the Italian region south of the 43^{0}N. In: Issar S. & Brown N. Eds., Water, environment and society in times of climatic change, (1998) 241-271.

[22] A. Farroni, M. Petitta, M. Tallini, Togna A., Indagine sull'Idrogeologia del Massiccio del Gran Sasso. Revisione dei dati esistenti e nuove considerazioni. Studi Geologici Camerti, Vol. Spec. (1999) 117-135.

[23] R. Massoli-Novelli, M. Petitta, Hydrogeological impact of the Gran Sasso tunnels (Abruzzi, Italy). In: Marinos P.G., Koukis G.C., Tsiambaos G.C. & Stournaras G.C. Eds., Engineering Geology and the Environment, **3** (1997) 2787-2792.

[24] R. Massoli-Novelli, M. Petitta, Le sorgenti del Parco Nazionale "Gran Sasso - Monti della Laga": il massiccio del Gran Sasso. In: Burri E. Ed., Aree protette in Abruzzo: contributi alla conoscenza naturalistica e ambientale, (1998) 9-34.

[25] R. Massoli-Novelli , M. Petitta, R. Salvati, Analysis and protection of groundwater resources: Capo Pescara karst springs (Central Italy). In: Fendekova M. & Fendek M. Eds., Hydrogeology and land use management (1999) 449-454.

[26] . Mazziotti Di Celso, M. Spizzico, M. Tallini, Studio idrochimico multitemporale delle acque sorgive dell'acquifero carsico del Gran Sasso (Italia centrale) per un affinamento del modello idrochimico concettuale. Proceedings of 2^{nd} Congresso Nazionale AIGA, Bari 15-17/02/2006, Giornale di Geologia Applicata, **2** (2005) 420-428.

[27] A. Monjoie, Hydrogeologie du massif du Gran Sasso (Apennin central). Coll. Pubbl. Fac. Scienze Appl. Univ., **53** (1975) 1-60.

[28] M. Petitta, R. Massoli-Novelli, Primi risultati del monitoraggio geoambientale delle sorgenti del Fiume Vera (Gran Sasso). Quaderni di Geologia Applicata, suppl.**1/95** (1995) 93-101.

[29] M. Petitta, R. Massoli-Novelli, Tirino springs (Abruzzi, Italy): an important groundwater resource for humans and environment. In: Van Brahana J., Eckstein Y., Ongley L.K., Schneider R. & Moore J.E. Eds, Gambling with groundwater, (1998) 97-103.

[30] M. Petitta, D. Ranalli, M. Tallini, Temperature and conductivity mapping for detecting groundwater flowpaths in karst aquifers (Gran Sasso, central Italy). In: Seiler K.P. & Wohnlich S. Eds., New approaches characterizing groundwater flow, 2, (2001) 303-1307.

[31] M. Petitta, M. Tallini, Idrodinamica sotterranea del massiccio del Gran Sasso (Abruzzo): indagini idrologiche, idrogeologiche e idrochimiche (1994-2001). Boll. Soc. Geol. D'It., **121** (2002) 343-363.

[32] M. Petitta, M. Tallini, Groundwater resources and human impacts in a Quaternary intramontane basin (L'Aquila Plain, Central Italy). Water International, **28** (2003) 57-69.

[33] Presidenza del Consiglio dei Ministri, La siccit in Italia, 1988-1990. Dipartimento Protezione Civile. Ufficio Coordinamento delle attivit di previsione e prevenzione, Servizio rischio idrogeologico, Roma, Istituto Poligrafico e Zecca dello stato, (1994) 1-193.

[34] M. Scozzafava, M. Tallini, Net infiltration in the Gran Sasso Massif (Central Italy): Thornthwaite water budget using the CN method (Soil Conservation Service). Hydrogeology Journal, **9** (2001) 461-475.

[35] Stigliano P., A. Altieri, R. Barberi, G. De Caterini, R. Massoli-Novelli, E. Miccadei, T. Piacentini, M. Petitta, R. Salvati, Studi per un monitoraggio idrologico del massiccio del Gran Sasso (Abruzzo). Studi Geologici Camerti, vol.spec. (1999) 153-170.

[36] M. Tallini, M. Petitta, Ranalli D., S. Tersigni, Karst aquifer characterization using physico-chemical spring data (Gran Sasso, Central Italy). In: Sililo O. et al. Eds., Groundwater: Past Achievements and Future Challenges, (2000) 629-634.